Evaluation of Phosphate Treatment and Long-Term RUNX2 Suppression on Adult Human MSC Chondrogenesis and Neo-Cartilage Formation

by

Tiana Jasmine Wong

A dissertation submitted in partial fulfillment
of the requirements for the degree of
Doctor of Philosophy
(Biomedical Engineering)
In The University of Michigan
2022

Doctoral Committee:

Professor Rhima Coleman, Chair
Professor Kurt Hankenson
Professor David Kohn
Professor Jan Stegemann

Tiana J. Wong

tjwong@umich.edu

ORCID iD: 0000-0001-9366-2393

DEDICATION

To my husband, Kyle, who has been my rock and an endless source of encouragement.

To Mom, 婆婆, and 公公 who have supported me from day one.

ACKNOWLEDGMENTS

I would like to first thank my thesis advisor, Dr. Rhima Coleman. I am beyond grateful for your guidance throughout my time at University of Michigan. You are an outstanding mentor that has helped me feel seen and heard during my graduate career. I greatly appreciate how you believed in me, even when I didn't believe in myself.

I would also like to thank my dissertation committee members, Dr. David Kohn, Dr. Jan Stegemann, and Dr. Kurt Hankenson, for their time, dedication, and insight towards this thesis project.

Thank you to members of the Coleman lab. Dr. Biming Wu, Dr. Kevin Miles, Sunny Karnan, Ciara Davis, Gurcharan Kaur, Dr. Yue Qin, Dr. Ryan Rosario, this thesis would not have been possible without all our discussions throughout the years.

Finally, I would like to extend thanks to the Bridge to Doctoral program for bringing me to Michigan.

TABLE OF CONTENTS

LIST OF FIGURES

LIST OF TABLES

ABSTRACT

Clinical repair strategies for articular cartilage defects are limited by the inability of the tissue to self-repair, often resulting in post-traumatic osteoarthritis (PTOA). PTOA arises from the degradation of structural cartilage extracellular matrix (ECM) proteins responsible for maintaining articular cartilage mechanics, such as aggrecan and collagen. Current cartilage tissue engineering strategies aim to utilize human-derived cells to regenerate cartilage prior to the onset of PTOA. Limited availability of chondrocytes – the primary cell type in articular cartilage – imposes a need for alternatives. Human mesenchymal stem cells (hMSCs) are a promising solution as they can be found in a variety of tissues and can differentiate into MSC-derived chondrocytes (MdChs). However, MSCs are limited by their inability to produce a stable chondrogenic phenotype and deposit and maintain ECM in long-term culture due to maturation, (hypertrophy) where metalloproteinases cleave collagen II and aggrecan. As a result, MSC-derived cartilage regeneration techniques are not yet suitable for clinical use. The **central objective** of this thesis is to increase cartilage matrix accumulation to develop more clinically functional cartilage tissue by increasing matrix deposition and stabilizing the chondrogenic phenotype of MSCs.

We investigated two approaches to increase cartilage ECM accumulation and improve MdCh-based cartilage tissue engineering functional outcomes: inorganic phosphate (Pi) treatment and RUNX2 suppression. First, we investigated the time and dose dependent response of Pi on MdCh chondrogenesis. We found that Pi increased cartilage ECM production, but also increased MdCh

hypertrophy and mineralization. Next, we evaluated the long-term matrix production of RUNX2 suppression on MdChs using our previously developed cell-regulated gene circuit. We found that the RUNX2 gene circuit increased cartilage matrix and stiffness of neo-cartilage tissues long-term. Finally, we evaluated the combinatorial effect of RUNX2 suppression and Pi treatment. We showed that combined treatment of Pi and RUNX2 suppression exhibited reduced MdCh hypertrophy but did not significantly increase matrix accumulation.

Overall, this dissertation explores methodologies that promote both cartilage matrix accumulation and reduces cartilage matrix loss during long-term culture to better support the use of MdChs in cartilage defect repair strategies.

CHAPTER 1 : Introduction

1.1 Background

Articular (hyaline) cartilage is the connective tissue that covers the end of the long bone and provides a smooth, low friction, articulating surface and redistributes load across the joint[1]. The cartilage extracellular matrix (ECM) deposited by chondrocytes is composed of collagen type II and aggrecan, which enables the unique mechanical function of cartilage (Fig. 1-1)[1]. Collagen type II is deposited by chondrocytes and forms a dense fibril network that creates the tensile strength of cartilage that resists tissue swelling[1]. Aggrecan contains negatively charged sulfated glycosaminoglycan (sGAGs) side chains which attracts water molecules into the tissue which provides cartilage with its compressive properties[1,2]. Within a healthy joint, the mechanical properties of the ECM protect healthy chondrocytes from mechanical stress.

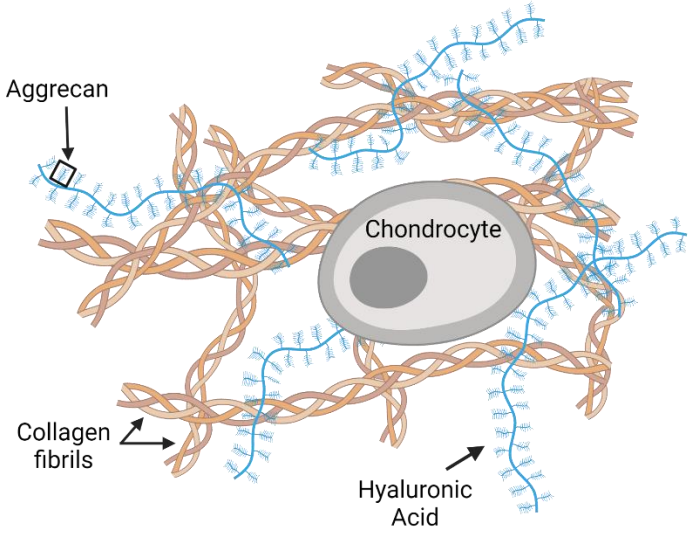

Created with BioRender.com

Figure 1-1. Schematic of articular cartilage matrix.

As a result of cartilage injury, there is an increase in tissue stresses, degradation enzymes, and inflammation in the joint, releasing collagen and aggrecan fragments as well as inflammatory cytokines such as tumor necrosis factor (TNF)-α and interleukins (ILs) into the synovium[3]. Inflammation upregulates the expression of RUNX2, the master transcription factor of hypertrophy that drives chondrocyte maturation and upregulates cartilage matrix-degradation enzymes[4]. Chondrocytes exposed to this suboptimal activated environment further upregulate the presence of inflammatory cytokines and drives the degradation of cartilage extracellular matrix. Cartilage is avascular and cannot self-repair due to lack of access to progenitor cells and nutrients[5]. Additionally, cartilage is aneural so injuries often go undetected until there is pain from inflammation or exposure of the underlying bone[6]. Long-term untreated injuries can result in post-traumatic osteoarthritis (PTOA)[7,8]. PTOA is a debilitating disease of the joint that results from trauma that affects over 5.6 million people within the United States[7,9]. Even with injury intervention, the risk of developing PTOA is between 20-50%[10].

1.2 Current Treatment Strategies

There are several common surgical procedures used to repair traumatic articular cartilage injuries including microfracture, osteochondral implantation, and autologous chondrocyte implantation[11].

Microfracture is a commonly performed repair technique for small cartilage defects[12]. Within this procedure, the defect site is cleaned of debridement and the underlying subchondral bone is perforated to recruit progenitor cells to the injury site for healing[13]. Bone marrow-derived mesenchymal stem cells (MSCs) recruited to the repair site forms new cartilaginous tissue[11]. The limitation of this method is that the microfracture is restricted to treatment of small defects (< 2mm) and recruited MSCs often create fibrocartilage rather than hyaline cartilage[12]. Unlike hyaline

cartilage, fibrocartilage is rich in collagen type I and does not have sufficient mechanical properties to resist high compressive loads of the knee joint[14,15]. As a result, degradation of tissue at the repair site can lead to onset of PTOA[11,14].

Osteochondral implantation is a clinical treatment that repairs cartilage defects with tissue grafts from healthy cartlilage[2,12]. The cartilage defect is cleaned and a cylindrical osteochondral plug, which contains a portion of the subchondral bone and cartilage, is removed from a non-load bearing portion of the knee and is transplanted to the defect site[12]. Limitations of this treatment option include limited availability of viable donor tissue and an increase in cartilage donor site morbidity[16]. There is also limited tissue integration between the healthy cartilage and the osteochondral plug because cartilage does not proliferate and travel within mature cartilage.

Autologous chondrocyte implantation (ACI) is a more recent treatment for large full-thickness defects[14]. First, a procedure is required to harvest healthy chondrocytes from a non-load bearing portion of the joint. The chondrocytes are then expanded *in vitro* prior to a second procedure[12]. During the second surgery, chondrocytes are implanted in the cartilage defect site and a membrane flap is placed on top to contain cells within the repaired region[12]. Benefits of this technique include use of the patient's own cells and positive long-term clinical outcomes[14]. However, autologous chondrocyte implantation is a multistep procedure and has longer recovery times[14]. To improve ACI outcomes, matrix autologous chondrocyte implantation (MACI) was developed to create more stable, biomechanical tissues faster. This method is similar to ACI, however, after *in vitro* expansion, chondrocytes are seeded onto a scaffold prior to implantation[12]. Like ACI, the limitation of this procedure is that it includes multiple invasive procedures and requires *in vitro* monolayer expansion of chondrocytes, which is not an ideal method of culturing

them since they are prone to dedifferentiation[17]. Due to the limitation of chondrocyte expansion and culture, alternative cell sources have been explored for cartilage tissue engineering.

1.3 Cartilage Tissue Engineering Efforts

Since current treatment options can be invasive and do not restore native tissue mechanics for cartilage tissue repair, tissue engineering strategies have been implemented to create new cartilage tissues. Aggrecan and collagen type II are the key structural macromolecules required for cartilage tissue mechanics[18,19]. Strategies to improve cartilage matrix deposition and create functional cartilage tissues include the use of various cell types, scaffolds, biomolecular and biomechanical stimuli[20–22].

Chondrocytes are the current gold standard for cartilage tissue engineering and are used in ACI and MACI cartilage treatments[12]. However, healthy chondrocytes needed for these procedures are limited since they can only be harvested from articular cartilage and tend to dedifferentiate during monolayer expansion[17,23]. Thus, alternative cell types have been explored for cartilage tissue engineering, such as mesenchymal stem cells[24].

Adult mesenchymal stem cells (MSCs) are a promising cell alternative for cartilage tissue engineering because they can differentiate into chondrocytes and are harvested from various tissues such as bone marrow and adipose tissue[24,25]. MSCs can follow lineages towards adipogenesis, chondrogenesis, and osteogenesis[26]. Like chondrocytes, MSC- derived chondrocytes (MdChs) produce cartilage matrix proteins like collagen type II and aggrecan (Fig. 1-2)[18,27,28]. Many studies have evaluated chondrogenic stimuli to induce and maintain MdCh chondrogenesis such as the administration of biomolecular and mechanical stimuli[2]. Common growth factors utilized for chondrogenic induction of MSCs, such as TGF-β, have shown to increase the production of cartilage ECM macromolecules[2]. Additionally, studies have shown that mechanical

stimuli, such as shear stress, dynamic compressive testing, and hydrostatic pressure, induce differentiation of MSCs and increase production of cartilage ECM[2,20,29].

1.4 *In vitro* Maturation of Human Mesenchymal Stem Cells

While MSCs are a promising alternative for primary chondrocytes for cartilage tissue engineering, the fact that MSCs do not have a stable chondrogenic phenotype remains a challenge[20,25,30]. MSCs when induced towards chondrogenesis follow the endochondral ossification pathway, a multi-step process that occurs during limb development [31–33]. During limb development, cells first condense prior to early chondrogenesis, where they mimic primary chondrocyte behavior[34]. Chondrocyte proliferation and matrix production lead to cartilage formation. Once chondrocytes stop proliferating, they continue towards hypertrophic maturation, calcification, and blood vessel invasion before differentiating into bone (Fig.1-2)[34]. While MdChs undergo chondrogenesis, they secrete collagen type II and aggrecan; however, with maturation, MdChs continue down the endochondral ossification pathway and begin to express hypertrophy-associated markers not expressed in primary chondrocytes.

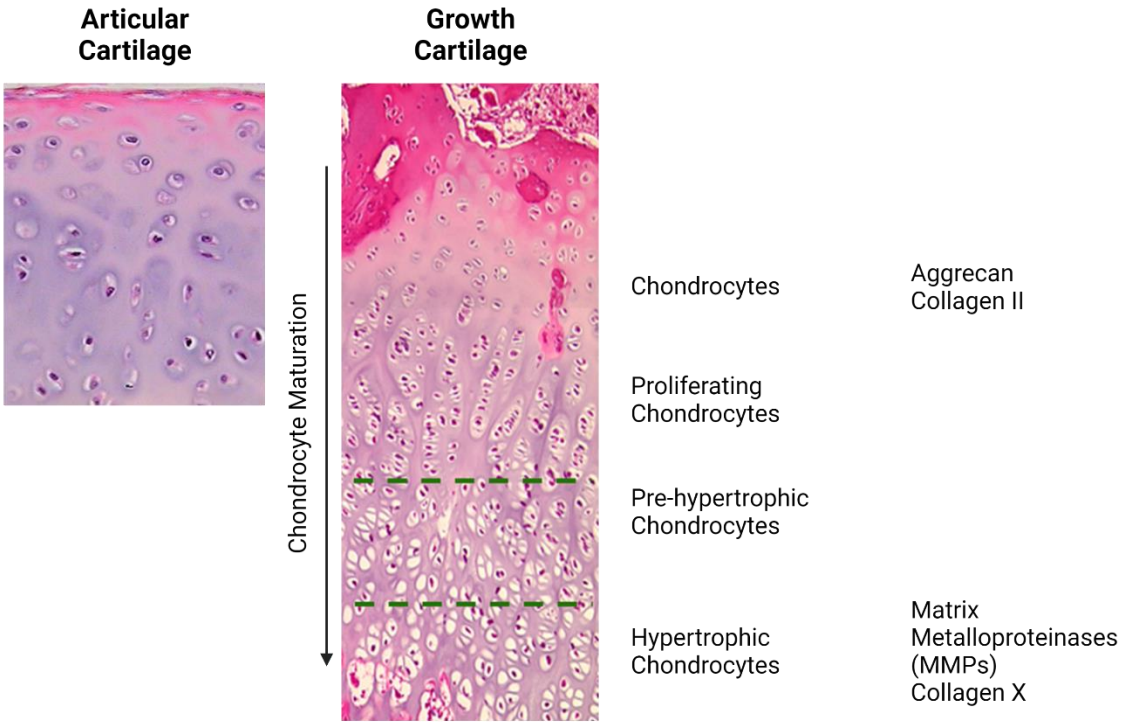

Figure 1-2. H&E staining of articular cartilage and growth cartilage.

During hypertrophy, RUNX2, the master transcription factor of hypertrophy is upregulated while SOX9, the master transcription factor for chondrogenesis is downregulated[35,36]. RUNX2 has many downstream effectors including collagen type X and matrix metalloproteinases (MMPs)[4]. MMPs cleave collagen fibrils into fragments, which compromises the tensile strength of the tissue[2]. Another metalloproteinase that is expressed during hypertrophy is a disintegrin and metalloproteinase with thrombospondin motifs (ADAMTSs)[1]. Since these components are the essential components of cartilage mechanics, inhibition of macromolecule degradation can improve the long-term outcomes of MdCh cartilage.

1.5 Osteoarthritis and Chondrocyte Maturation

Osteoarthritis (OA) and cartilage injuries can lead to an activated joint, defined by the elevation of calcification and/or inflammatory factors. Osteoarthritic joints have elevated alkaline phosphatase (ALP) activity and inorganic phosphate (Pi) levels. Additionally, inorganic phosphate is one of the required molecules for hydroxyapatite formation during mineralization of extracellular matrix and increases as chondrocytes mature[37]. The available phosphate binds with calcium to create calcium-phosphate complexes that are found in 60% of moderate OA cases[38]. Upregulation of Pi during osteoarthritis and cartilage injury contributes to the formation of basic calcium phosphate (BCP) crystals which drives cartilage degradation[39]. BCPs are known to activate macrophages, synovial fibroblasts, and increase MMPs, which further propagates cartilage degradation and drives chondrocyte maturation[40]. Since all neo-tissue constructs used to treat defects are exposed to an activated environment, which drives expression of hypertrophic induction, it is an important element to consider for cartilage tissue repair.

1.6 Genetic Engineering in Cartilage Tissue Regeneration

Gene silencing works to prevent expression of specific genes of interest. Gene silencing allows for precise targeting of therapeutic pathways[41]. One method to implement gene silencing is through RNA interference (RNAi). RNAi is a sequence-specific multi-step process that leads to targeted degradation or suppressed translation of mRNAs[41]. RNAi has been investigated for diseases such as cancer and viral infections[42].

Various research groups have shown that use of RNAi can be used to inhibit hypertrophy of MSCs during chondrogenic differentiation. siRNA can be transient and long-term inhibition of genes will be difficult, especially *in vivo*[41]. Lentiviral delivered short hairpin RNA (shRNA) is a promising solution to this problem since it integrates into the genome of the cell and can be passed

onto daughter cells. Unlike siRNA, shRNA contains a hairpin structure due to the short loop region flanked by complementary siRNA sequences[41]. During RNAi, the shRNA is processed into siRNA that induces silencing of the target sequence. Basic shRNAs are expressed using Pol III promoter and have high results of cytotoxicity, especially in mammalian cells[41,43,44]. Through this shRNAs are processed through natural occurring miRNA pathways, reducing cytotoxicity[41]. These miRNA-based shRNAs are also expressed by Pol II promoters, enabling use of tissue- specific mammalian promoters to induce gene silencing in various types of cells[43].

1.7 Project Goals and Hypothesis

The central objective this thesis is to increase cartilage matrix accumulation and to stabilize the chondrogenic phenotype of MSCs for more clinically functional cartilage tissue. The following work investigates two methodologies to improve cartilage matrix accumulation. The first method evaluates the cell-state and dose-dependent response of MdChs during chondrogenesis. The second method evaluates the long-term effects of our previously established cell-autonomous shRUNX2 gene circuit on MdCh cartilage matrix accumulation and resultant compressive mechanics. Lastly, we investigated whether the combinatorial treatment of these two methods would result in increased cartilage matrix accumulation. We hypothesize that Pi treatment during chondrogenesis and chondrocyte maturation will increase cartilage matrix accumulation in a dose-dependent manner and that Pi treatment in conjunction with RUNX2 suppression will further increase the accumulation of articular cartilage structural macromolecules to create functional cartilage tissue. We will investigate this hypothesis with the following aims:

Aim 1: Determine the concentration and cell-state-based effects of β-glycerophosphate on mesenchymal stem cell chondrogenesis.

One method to induce hypertrophy in MSCs is to introduce β-glycerophosphate (βGP) to the culture medium to increase inorganic phosphate (Pi). Studies have shown that Pi has cell-state-dependent effects on chondrogenesis where it can promote either chondrogenesis or maturation and mineralization[39,45–48]. In this aim, we evaluate the cell-state and dose-dependent response of Pi on MdCh chondrogenesis. The main objective of this aim was to determine whether Pi can be used to increase cartilage matrix accumulation.

Aim 2: Evaluate the effects of long-term RUNX2 suppression on MSC chondrogenesis and cartilage matrix accumulation.

Our lab previously developed a cell-autonomous gene circuit that drives the expression of short hairpin RNA (shRNA) for RUNX2 (shRUNX2) with expression of intracellular RUNX2. Wu et al has shown that the use of this gene circuit improves MdCh cartilage matrix accumulation[49]. However, the long-term efficacy of this gene circuit on adult human MdCh chondrogenesis and the mechanical response has not yet been evaluated. The purpose of this study was to evaluate the long-term efficacy of our cell-autonomous gene circuit on MdCh chondrogenesis and to determine whether RUNX2 suppression alone is sufficient to create functional cartilage tissue.

Aim 3: Investigate the cumulative effects of Pi treatment and auto-regulated RUNX2 suppression on MSC-based cartilage matrix accumulation.

Aims 1 and 2 investigated two methods to improve cartilage matrix accumulation; however, our findings showed that Pi levels that increased cartilage matrix accumulation also increased tissue mineralization while RUNX2 suppression decreased expression of MdCh hypertrophic markers. Therefore, we investigated whether the combinatorial treatment of Pi and

RUNX2 suppression. First, we investigated whether combined RUNX2 inhibition and Pi treatment would result in higher matrix accumulation and reduce Pi-induced hypertrophy in neo-tissues. Second, we investigated whether Pi priming increases cartilage matrix accumulation prior to exposure to a high Pi activated environment.

CHAPTER 2 : Inorganic Phosphate Increases Cartilage Matrix Accumulation During Mesenchymal Stem Cell Chondrogenesis

2. 1 Introduction

Mesenchymal stem cells (MSCs) have been a promising alternative for cartilage tissue engineering due to their multipotent capacity[50]. Significant efforts have been made in the tissue engineering field to optimize articular cartilage extracellular matrix production by MSC-derived chondrocytes (MdChs). However, MSC-based cartilage tissue regeneration is limited by the instability of the chondrogenic phenotype and the hypertrophic induction of MdChs, a cartilage maturation process often associated with osteoarthritis (OA)[51]. In OA, chondrocytes are subjected to high-magnitude mechanical stresses, sustained inflammation, and an increase in mineral crystals that induces the hypertrophy of MdChs[47,52,53]. Exposure of MSC-derived chondrocytes to this activated environment can result in matrix loss and mineralization; therefore, it is critical to study the effect of these factors on tissue engineered cartilage[52,54].

Inorganic phosphate (Pi) is a signaling molecule that has been shown previously to mediate chondrocyte fate. Pi has been used extensively to induce hypertrophic maturation and mineralization of chondrogenic and osteogenic cells, such as ATDC5s and MC3T3, in *in vitro* studies of endochondral ossification [55,56] . Previously, we have shown that showed that early moderate Pi abundance enhanced early chondrogenesis of the mouse teratocarcinoma cell line ATDC5, resulting in higher aggrecan and collagen II expression. Conversely, late treatment with Pi inhibited chondrogenic differentiation and increased mineralization in these cells[46]. These

results suggest that the effect of Pi on chondroprogenitor cells is cell-state dependent and can have profound effects on their ECM production and maturation down the endochondral ossification pathway, which influences the composition of the ECM during cartilage repair.

In advanced stages of OA, there is an increase in alkaline phosphatase (ALP) activity within both the synovial serum and articular chondrocytes. ALP cleaves pyrophosphate (PPi) to release inorganic phosphate, which has been found to further propagate the deterioration of cartilage[57]. Specifically, the increase in available Pi often leads to the formation of calcium-phosphate crystal complexes by hypertrophic chondrocytes as OA progresses[58–61]. This in turn stimulates the production of matrix metalloproteinases like MMP3 and MMP13 by mature chondrocytes[48]. As such, any cell-based repair strategies introduced into this osteoarthritic environment are subjected to exposure to Pi; however, the role Pi plays on MdCh ECM production has not been widely explored. To design adjuvant therapies to resist these effects, we need a clearer understanding of the effect of Pi on MdChs. Therefore, the purpose of this study is to evaluate the temporal and dosage effects of Pi on MSC chondrogenesis and progression of MdCh hypertrophy.

2.2 Methods

2.2.1 Cell Culture

2.2.1.1 Cell Expansion

Bone Marrow-derived MSCs were gifted by Dr. Rodrigo Somoza in collaboration with CWRU Center for Multimodal Evaluation of Engineered Cartilage (CMMEC, Cleveland, Ohio). Cells were initially seeded at a density of 4,000 cells/cm^2. MSCs were expanded in monolayer in expansion media (Low glucose Dulbecco's modified Eagle's medium (DMEM) (Invitrogen), 10% Fetal Bovine Serum (Invitrogen), 1% Antibiotic-Antimycotic (Invitrogen), and 10ng/ml Fibroblast Growth Factor (FGF) (Shenandoah). At 80% confluency, cells were lifted using 0.25% Trypsin-

EDTA (Invitrogen) and neutralized using a solution composed of 10% Fetal Bovine Serum (Invitrogen) and 90% low glucose DMEM (Invitrogen). Cells were replated at a seeding density of 4,000 cells/cm^2 until a population doubling of 11 is reached.

2.2.1.2 Chondrogenic Differentiation and Treatment

Cell pellets were created by placing $2.5x10^5$ cells in chondrogenic media to U bottom 96 well plates (ThermoFisher) and centrifuged at 1640 RPM for 5 minutes to condense cells. Pellets were cultured in chondrogenic media at 37°C at 5% CO_2. Chondrogenic pellet culture medium consisted of high glucose Dulbecco's Modified Eagles Medium (Gibco), 1% ITS+ Premix (Corning), 1% Non- essential amino acids (Gibco), 1% antibiotic-antimycotic (Invitrogen), 40µg/ml L-proline (Sigma), 50 µg/ml ascorbic acid 2- phosphate (Sigma), 0.1µM dexamethasone (Sigma), and 10ng/ml TGF-β1 (Shenandoah)[62]. Pi treatment groups received 0, 5, 10, or 20mM of βGP at varying time points of chondrogenesis (Fig. 1). Early treatment pellets were treated from days 0-14 of chondrogenesis, late treatment pellets were treated from days 14-28, and continuous treatment pellets were treated from days 0-28 (Figure 2-1).

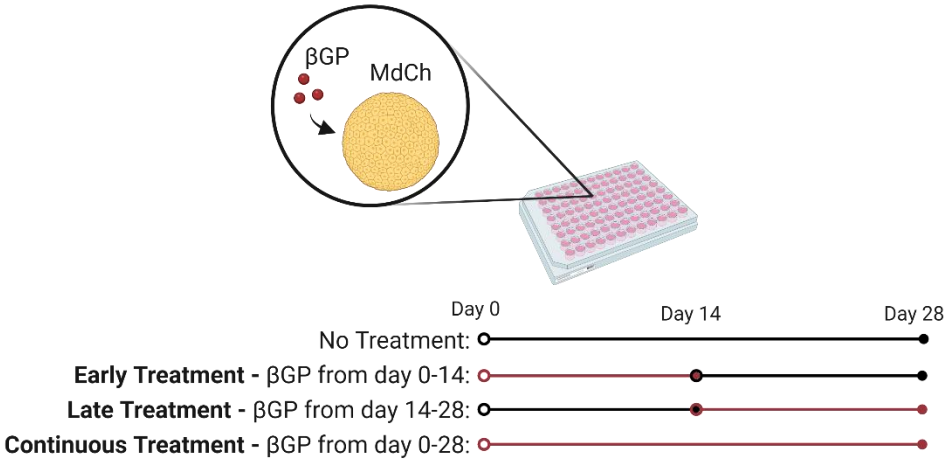

Created with BioRender.com

Figure 2-1. Experimental design. MdCh pellets were treated with 0, 5, 10, or 20mM of βGP from days 0-14 (early treatment), from days 14-28 (late treatment), or from days 0-28 (continuous treatment).

2.2.2 Biochemical Analysis

Pellets were harvested and digested using a 0.3 units/ml papain, cysteine, EDTA, and sodium phosphate solution. Digestion buffer was added to each sample prior to digestion at 65°C for 16 hours. Cartilage matrix accumulation was measured using the 1,9-dimethylmethylene blue (DMMB) assay as previously described[21]. Samples and chondroitin sulfate standards were diluted in papain buffer. Samples were run in triplicate in a clear flat bottom 96 well plate with DMMB dye and read at wavelengths 525nm and 595nm. Matrix production was normalized by DNA content as determined using the PicoGreen assay (Thermo Fisher). Diluted samples and λ DNA standards were run in triplicate in a black flat bottom 96 well plate with PicoGreen-Tris solution and read at excitation wavelengths 498nm and emission wavelength 528nm.

2.2.3 Histological analysis

Pellets were washed twice with PBS and fixed with 10% neutral buffered formalin at room temperature for 30 minutes. Fixed pellets were washed with PBS followed by 70% ethanol. Pellets

were dehydrated with an ethanol-xylene series prior to paraffin embedding and sectioning. Sections were deparaffinized and stained with Alcian Blue (1% in 3% Acetic Acid, Poly Scientific) and counterstained with Nuclear Fast Red (Electron Microscopy Sciences) to evaluate proteoglycan accumulation. Calcium deposition was visualized using a 2% Alizarin Red S dye (pH 4.3, Sigma). For immunofluorescence, sections underwent antigen retrieval (BD Pharmingen) and blocking prior to primary antibodies incubation for aggrecan (1:500 dilution in 10% Goat serum in 0.1% TBS-TX100), collagen type II (1:100), collagen type X (1:100), RUNX2 (1:100), or MMP13 (1:200) (Abclonal) overnight at 4˚C. Histological slides were incubated with secondary antibodies for 1 hour at room temperature Sections were counterstained with DAPI (Life Technologies) for 5 minutes at room temperature.

2.2.4 Gene Expression

Analysis of gene expression was performed as previously described[49]. Briefly, total RNA of pellets was isolated using TRI Reagent RT (Molecular Research Center). cDNA was synthesized using High-Capacity cDNA Reverse Transcription Kit (Life Technologies) and amplified using SYBR Green PCR Master Mix (Life Technologies) on Applied Biosystems 7500 Fast well plates. The mean cycle threshold of housekeeping genes *GUS* and *TBP* (Ct_{hk}) was used to determine the fold change of gene expression levels compared to day 0 samples using the $\Delta\Delta C_T$ method. Relative expression levels were calculated as $x = 2^{-\Delta\Delta C_T}$, where $\Delta\Delta C_T = \Delta T - \Delta C$, $\Delta T = (Ct_{exp} - Ct_{hk})_t$, and $\Delta C = (Ct_{exp} - Ct_{hk})_{t0}$.

Table 2-1. Primer sequences for qPCR gene expression analysis.

Gene	Forward	Reverse
ACAN	GGAGTGGATCGTGACCCAAG	AGTAGGAAGGATCCCTGGCA
COL2A1	CTCCAATGGCAACCCTGGAC	CAGAGGGACCGTCATCTCCA
RUNX2	CCGGAATGCCTCTGCTGTTA	AGCTTCTGTCTGTGCCTTCTGG

COL10A1	GAACTCCCAGCACGCAGAATC	TGTTGGGTAGTGGGCCTTTT
MMP13	TTGCAGAGCGCTACCTGAGA	CCCCGCATCTTGGCTTTTTC
OCN	CTCACACTCCTCGCCCTATTG	CTTGGACACAAAGGCTGCAC
ALP	GTAAGGACATCGCCTACCAG	GGCTTTCTCGTCACTCTCAT
TBP	GTGGGGAGCTGTGATGTGAA	TGCTCTGACTTTAGCACCTGT
GUS	GACTGAACAGTCACCGACGA	ACTTGGCTACTGAGTGGGGA

2.2.5 Phosphate Concentration Analysis

Cell culture media from each condition was collected during media changes. Samples were diluted 1:20 or 1:50 with water based on Pi treatment condition prior to analysis. Phosphate concentration levels were assessed in the culture medium using the QuantiChrom™ Phosphate Assay Kit (BioAssay Systems). 50µl of samples and standards were pipetted into a 96-well plate prior to the addition of 100µl of assay reagent. The plate was incubated at room temperature for 30 minutes. Phosphate concentrations were determined by reading at an optical density of 620nm and calculations using equation from the manufacturer's protocol.

2.3 Results

To elucidate the cell-state-dependent response of Pi on MSC chondrogenesis, we first monitored Pi concentration within the media at different cell states of chondrogenesis to calculate the concentration available in cultures on a per cell basis, which we term Pi abundance (Pi/DNA; Fig. 2-2). Pi abundance levels were categorized as Low (Pi/DNA < 70 µg/µg), Medium (Pi/DNA = 70µg/µg – 175µg/µg), and High (Pi/DNA > 175µg/µg).

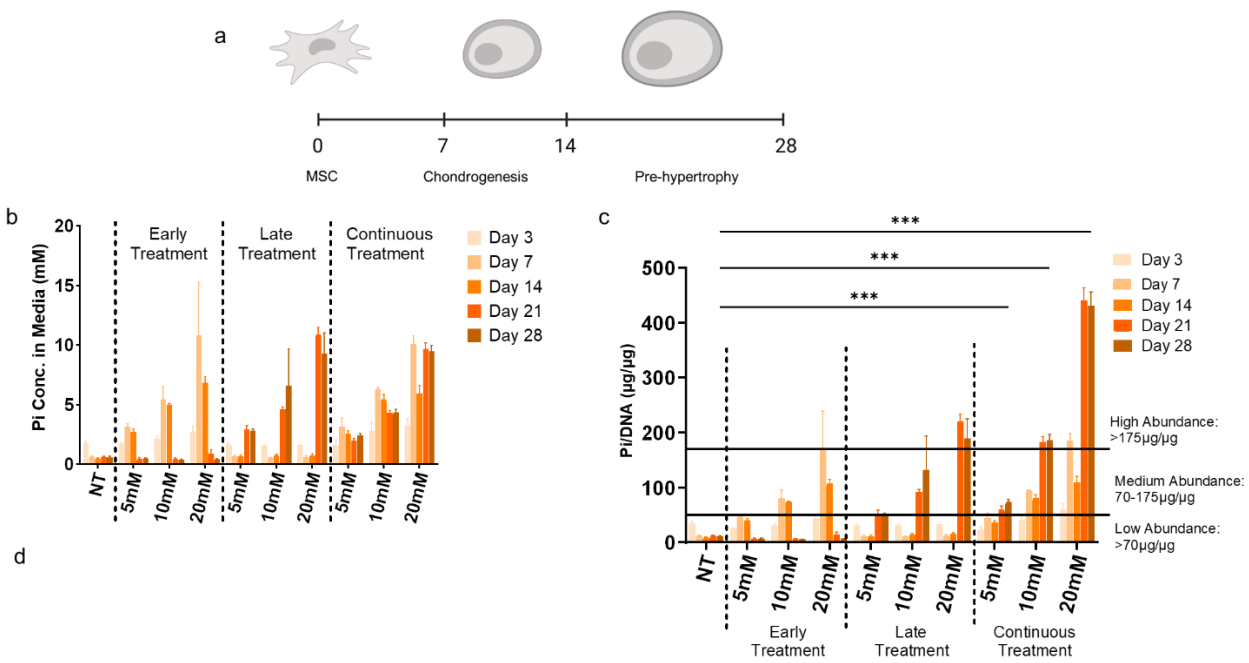

Figure 2-2. Upregulation of Pi abundance at different time points of chondrogenesis. (a) Time course of MSC chondrogenesis. (b) Pi concentration within culture media over time course of chondrogenesis. (c) Pi abundance based on varying concentrations and time points (*** indicates p-value < 0.01).

Pi abundance increases matrix accumulation in a state-dependent manner. Continuous high Pi abundance levels correlated with increased levels of cartilage matrix production. By day 28, sGAG content was increased by 120.6%, 169%, and 183.2% in low, medium, and high Pi abundance, respectively, compared to non-treated MdChs (Fig. 2-3a). This is further supported by Alcian blue staining where we observe rich abundance staining at day 28 of culture (Fig. 2-3b). However, moderate and high Pi abundance pellets also exhibit mineralization as determined through Alizarin Red staining (Fig. 2-3c).

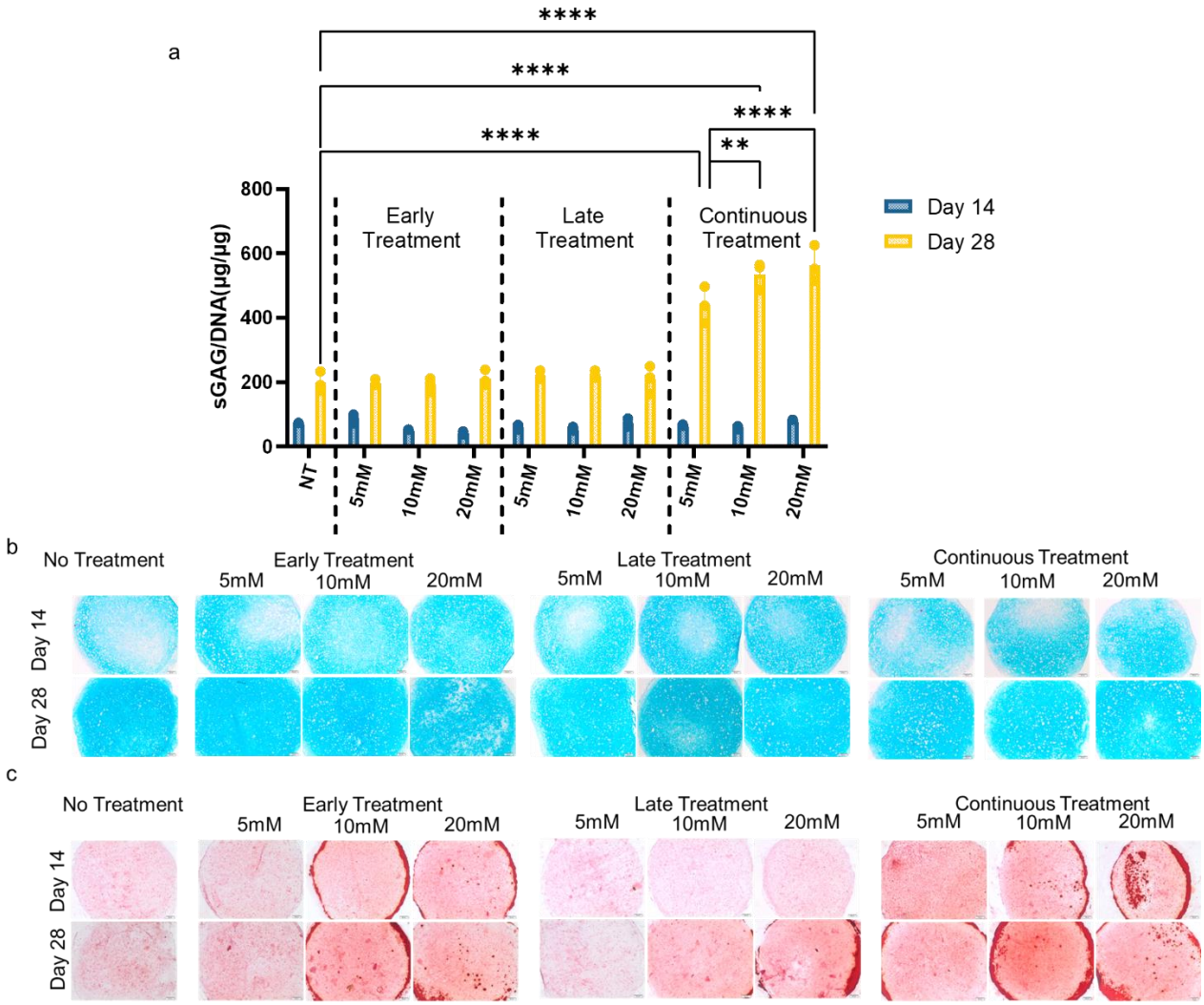

Figure 2-3. Cartilage matrix accumulation at day 14 and day 28 of chondrogenesis. (a) sGAG quantification based on biochemical DMMB analysis normalized by DNA (** indicates p-value = 0.0017, **** indicates p-value < 0.0001). (b) Alcian blue stain to for articular cartilage matrix accumulation. (c) Alizarin red stain to show mineralization of pellets.

Gene expression of collagen type II was upregulated with low Pi abundance during early chondrogenesis, but there was no effect on aggrecan gene expression (Fig. 2-4a, b). Collagen type II protein expression was upregulated with early low Pi abundance but decreased with high Pi abundance at day 14 (Fig. 2-4d). By day 28, collagen type II expression was increased compared to non-treated MdChs (Fig. 2-5a). Aggrecan protein expression was elevated with Pi treatment at day 14 as shown with abundant and dispersed immunofluorescence (Fig. 2-5b). However, by day

28 aggrecan staining for all conditions became more localized, especially with those treated continuously with Pi (Fig. 2-5b).

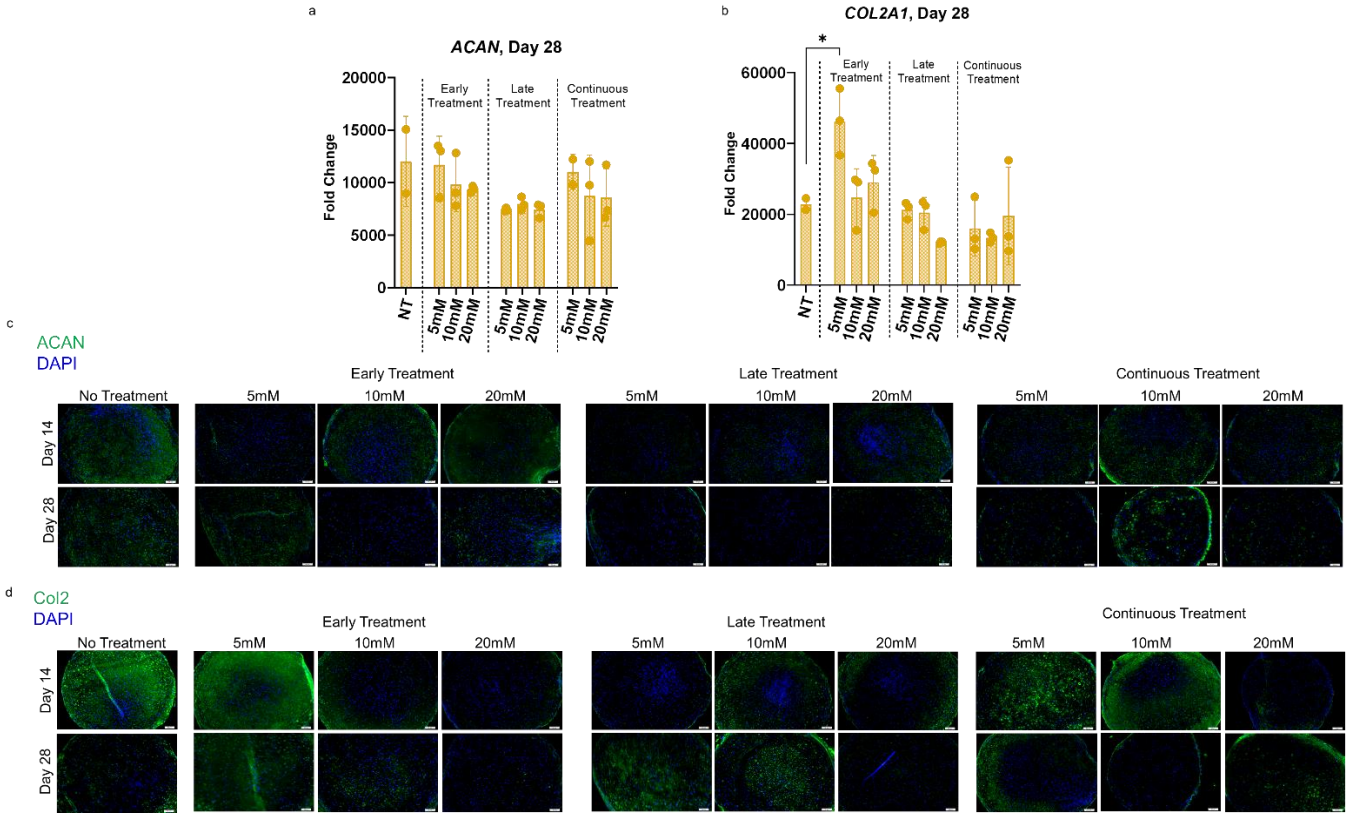

Figure 2-4. Chondrogenic gene and protein expression of culture in response to Pi abundance. Gene expression of chondrogenic markers (a) collagen type II (* indicated p = 0.0127) and (b) aggrecan were evaluated at day 28. Immunofluorescence shows protein expression of chondrogenic markers (c) collagen type II and (d) aggrecan decreased with high Pi abundance by day 28 of chondrogenesis but increased with lower levels of Pi abundance.

Pi did not significantly alter gene expression of hypertrophic markers RUNX2, collagen type X, MMP13, osteocalcin, and ALP (Fig. 2-5). However, high Pi abundance increases protein expression of hypertrophic and osteogenic markers (Fig. 2-5d, e, f). MdChs with moderate and high Pi abundance during early chondrogenesis exhibited higher expression of hypertrophic markers than those treated during late chondrogenesis. This suggests that early Pi treatment is responsible for the promotion of hypertrophic induction.

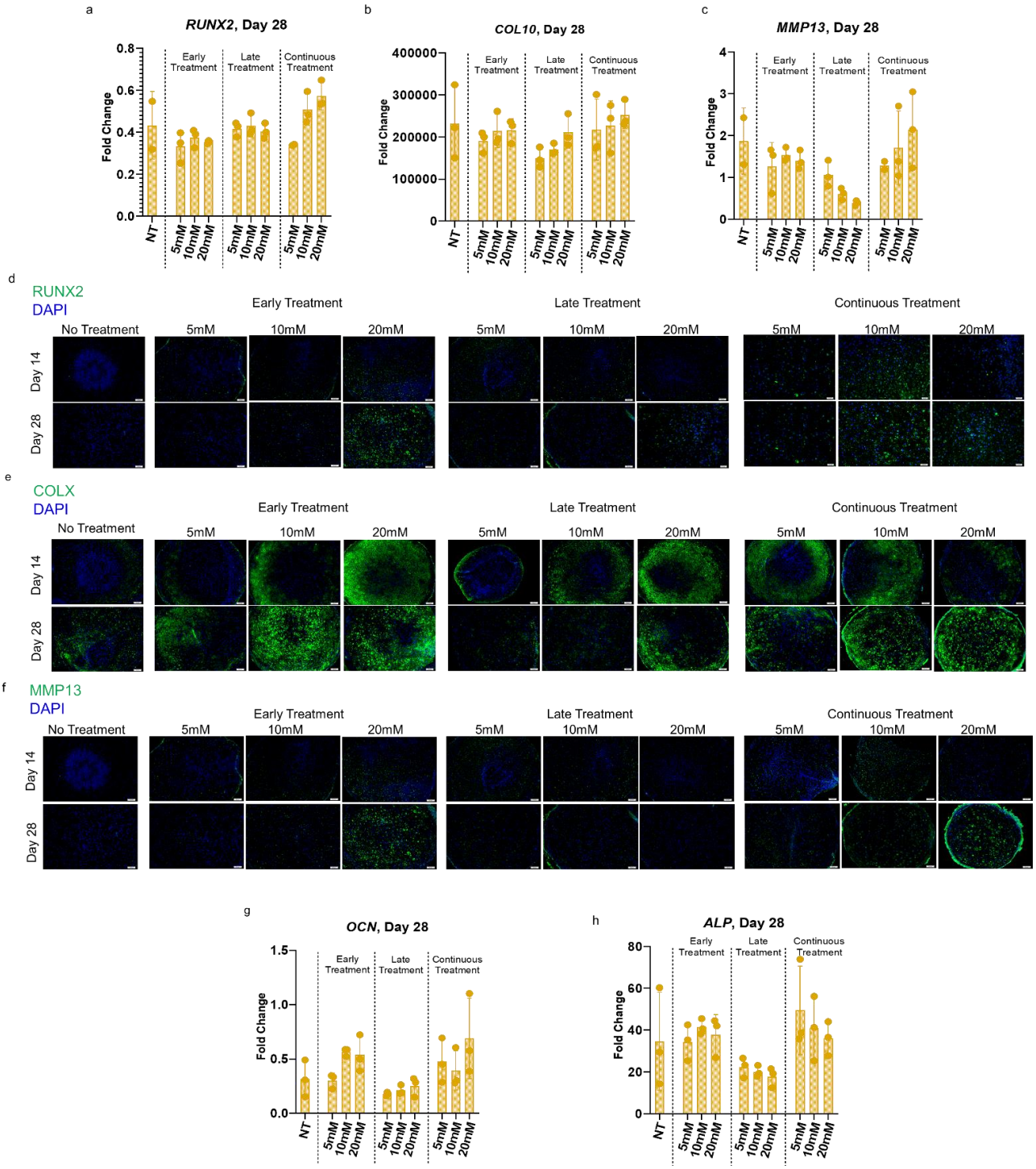

Figure 2-5. Hypertrophic gene and protein expression of culture in response to Pi abundance. Gene expression of hypertrophic markers (a) RUNX2 and downstream targets (b) COL10 and (c) MMP13. Protein expression shown through immunofluorescence, shows hypertrophic transcription factor, (d) RUNX2, and downstream targets (e) ColX and (f) MMP13 were

elevated with increased Pi abundance. Gene expression of g) Osteocalcin and (h) ALP increase show no significant change with Pi treatment.

2.4 Discussion

This study of hMdChs shows that cartilage matrix accumulation and hypertrophic induction are dependent on both Pi abundance and cell state. We first showed that Pi abundance varies with the concentration of βGP and the time of administration. Twenty millimolar βGP and continuous treatment of βGP resulted in high Pi abundance (Pi/DNA> 175μg/μg) which exhibited the most significant effect on cartilage matrix accumulation as shown through DMMB and Alcian Blue staining. Low Pi abundance increased COL2A1 expression with early treatment and had no significant increase in hypertrophic markers such as ColX, RUNX2, and MMP13. Together, these results indicate that low continuous Pi treatment would provide improved cartilage matrix outcomes for cartilage tissue engineering. Additionally, continuous βGP treatment has a cumulative effect on available Pi levels and is an important factor when providing βGP to MdChs.

These findings are contrary to the findings of the ATDC5 response to Pi found by Wu et. al., which showed decreased sGAG quantities with continuous high treatment[46]. However, high Pi abundance also corresponded with elevated expression of hypertrophic markers RUNX2, COL10A1, and MMP13, and increased tissue mineralization. This is consistent with previous literature that shows that Pi increases ColX expression and induce mineralization[46,61] and studies that have utilized Pi to induce hypertrophy of hMdChs[63]. While high Pi increases mineralization within MdChs, it does not appear that Pi inhibits induction of early chondrogenesis and does not increase cartilage matrix loss by day 28 of chondrogenic culture. This could be due to the prolonged chondrogenic timeline of MdChs compared to chondrogenic cell lines. Therefore, long-term chondrogenic studies should be performed to evaluate the full response of Pi on MdCh chondrogenesis on matrix loss and progression of chondrogenic gene expression.

As expected from previous literature, we observed an increase in RUNX2 protein expression and the expression of downstream RUNX2 targets as a response to high Pi abundance. This phenotypic change confirms a method to expedite hypertrophy and provides a foundation to evaluate MdCh phenotype stabilization techniques within a shortened time span. This is expected as Pi upregulates several cell-signaling pathways, such as ERK1/2, p38, and NFκB pathways, that may facilitate the phenotypic changes and hypertrophic induction of MdChs[52,64]. Upregulated hypertrophic factors, in addition to mineral deposition, due to elevated Pi levels are not ideal for articular cartilage-specific tissues as they increase inflammatory markers and progress cartilage degradation[48]. Furthermore, during cartilage injury treatments, MdChs are often inserted into activated joints which would increase their exposure to inflammatory factors and calcium phosphate complexes. Exposure to the activated environment would also drive hypertrophic induction and mineralization of MdChs, driving the progression of post-traumatic osteoarthritis. Therefore, while it may be beneficial to treat cells with Pi to increase cartilage matrix accumulation, steps must be taken to inhibit hypertrophic differentiation and mineralization. For example, our lab has previously developed a cell-autonomous gene circuit that works to stabilize the MdCh chondrogenic phenotype and reduce the expression of hypertrophic factors[49]. To improve overall cartilage matrix outcomes, such as increased chondrogenic markers and sGAG quantification, it would be beneficial to investigate the combined effects of Pi treatment and inhibition of hypertrophy on cartilage matrix production. Additionally, the result of this study introduces the notion of pre-conditioning MdChs to reduce he hypertrophic effects of Pi.

CHAPTER 3 : Long-Term Suppression of RUNX2 During MSC-Based Cartilage Formation Increases Cartilage Matrix Accumulation

3. 1 Introduction

Due to the avascular nature of articular cartilage, traumatic cartilage injuries can lead to post-traumatic osteoarthritis (PTOA), a painful and debilitating joint disease, if left untreated[2,7]. Current treatment options for these cartilage defects include microfracture, osteochondral implantation, and autologous chondrocyte implantation. Microfracture recruits progenitor cells from the underlying bone to the defect to facilitate cartilage repair[65]. However, this method results in the formation of fibrocartilage, a dense fibrous tissue rich in collagen type I, rather than articular cartilage[66]. Osteochondral implantation takes a plug from a non-load bearing portion of the knee to repair the cartilage defect[67]. However, there are various problems with this method, such as limited donor tissue and donor site morbidity[16]. Autologous chondrocyte implantation is a cell-based cartilage repair strategy that harvests chondrocytes from cartilage tissue and expands them in vitro before reimplantation back into the defect. While this method has positive clinical outcomes, this method is limited by the isolation of viable chondrocytes from the cartilage and requires multiple surgeries[68]. In addition, when chondrocytes are expanded *in vitro*, they dedifferentiate, expressing a fibrocartilage-like phenotype[69]. Due to these limitations, the use of adult human mesenchymal stem cells (MSCs) has been explored as an alternative cell source for cartilage tissue engineering.

MSCs are commonly explored for cartilage tissue engineering strategies but are limited by their ability to maintain a stable chondrogenic phenotype for long-term cartilage repair. Adult MSCs can differentiate along various lineages to become adipocytes, osteocytes, and chondrocytes[70]. After initial chondrogenic induction, MSC-derived chondrocytes (MdChs) are similar to primary articular chondrocytes in that they secrete cartilage matrix proteins such as collagen type II and aggrecan into the extracellular matrix (ECM) which play integral roles in cartilage mechanics[1]. However, MdChs continue down the endochondral ossification pathway leading to end-stage chondrocyte maturation (hypertrophy)[63,71]. At this stage, MdChs upregulate the master transcription factor for hypertrophy RUNX2. RUNX2 expression drives expression of cartilage degradation proteins such as matrix metalloproteinase-13 (MMP13) and aggrecanases that degrade the accumulated collagen type II and aggrecan within the extracellular matrix, compromising the mechanical integrity of the tissue[1,63].

Maintaining the chondrogenic phenotype and improving cartilage matrix accumulation has been a longstanding challenge within the field of cartilage tissue engineering. Various methods have attempted to address this issue. For example, studies have shown that MSCs cultured in hypoxic conditions experienced enhanced chondrogenesis compared to their normoxic (20% oxygen) counterparts, expressing higher sGAG levels and collagen type II[72–74]. Mechanical loading has been shown to decrease MMP expression[75], inhibit IL1-associated matrix degradation, and dynamic mechanical loading during chondrogenic culture has shown effectiveness in increasing cartilage matrix compared to free swelling environments[20]. Despite these efforts, MdChs are still unstable within long-term culturing conditions.

Genetic reprogramming has been utilized within cartilage tissue engineering to regulate the expression of genes to delay hypertrophic maturation[42,49]. Gene silencing through RNA

interference (RNAi) allows integration with the genome and can provide long-term inhibition of genes [41]. Our lab previously developed a cell-autonomous gene circuit that drives the expression of short hairpin RNA (shRNA) for RUNX2 (shRUNX2) with intracellular RUNX2 expression. This system is tunable through the implementation of varying amounts of cis enhancers upstream of the basal promoter. Wu et al have shown that the use of this gene circuit improves MdCh cartilage matrix accumulation[49]. However, the long-term efficacy of this gene circuit system in adult human MSCs has not yet been evaluated. The purpose of this study was to evaluate the long-term efficacy of our cell-autonomous gene circuit.

3.2 Methods

3.2.1 Cell Culture

3.2.1.1 Cell Expansion

Bone Marrow-derived MSCs were gifted by Dr. Rodrigo Somoza in collaboration with CWRU Center for Multimodal Evaluation of Engineered Cartilage (CMMEC, Cleveland, Ohio). Cells were initially seeded at a density of 4,000 cells/cm^2. MSCs were expanded in monolayer in expansion media (Low glucose Dulbecco's modified Eagle's medium (DMEM) (Invitrogen), 10% Fetal Bovine Serum (Invitrogen), 1% Antibiotic-Antimycotic (Invitrogen), and 10ng/ml Fibroblast Growth Factor (FGF) (Shenandoah). At 80% confluency, cells were lifted using 0.25% Trypsin-EDTA (Invitrogen) and neutralized using a solution composed of 10% Fetal Bovine Serum (Invitrogen) and 90% low glucose DMEM (Invitrogen). Cells were replated at a seeding density of 4,000 cells/cm^2 until a population doubling of 12 was reached.

3.2.1.2 Transduction

Cells were transduced with our previously developed auto-regulatory gene circuit that

suppresses RUNX2 levels by 80%[76]. Cells were exposed to the lentiviral supernatant (MOI of 5) with polybrene in the absence of antibiotics for 24 hours[49]. After lentiviral was removed, cells were washed with PBS. Transduced cells were selected using 1μg/ml puromycin (Sigma) and expanded in monolayer before being seeded into pellet culture.

3.2.1.3 Chondrogenic Differentiation

Pellets were seeded by adding $2.5x10^5$ cells suspended in chondrogenic media in each well of a U bottom 96 well plates (ThermoFisher) and centrifuged at 1640 RPM for 5 minutes. Pellets were cultured in chondrogenic media at 37°C at 5% CO_2. Chondrogenic pellet culture medium consisted of high glucose Dulbecco's Modified Eagles Medium (Gibco), 1% ITS+ Premix (Corning), 1% Non-essential amino acids (Gibco), 1% antibiotic-antimycotic (Invitrogen), 40μg/ml L-proline (Sigma), 50 μg/ml ascorbic acid 2- phosphate (Sigma), 0.1μM dexamethasone (Sigma), and 10ng/ml TGF-β1 (Shenandoah)[62].

3.2.1.4 Construct Preparation

Four percent low-gelling agarose was made by dissolving agarose (Sigma) in Phosphate Buffered Saline (PBS) (Invitrogen). Transduced MSCs were embedded in 4% low-gelling agarose at a 1:1 ratio to create 2% agarose cellular hydrogel to obtain a cell density of 20 million cells/ml. Hydrogels were maintained in chondrogenic media containing 10ng/ml TGF-β for the entire culture period.

3.2.2 Luciferase Assay

Luciferase activity of pellets were measured in 96 well plates at every media change. Chondrogenic media was replenished six hours prior to luciferase measurement. D-Luciferin (Biovision) was added to culture media thirty minutes before readings and incubated at 37°C.

Luminescence was measured using the SYNERGY H1 microplate reader (BioTek). Chondrogenic culture media was changed after readings.

3.2.3 Biochemical Analysis

Pellets were harvest on days 35, 56, and 70. A digestion buffer was made using a 0.3 units/ml papain, cysteine, EDTA, and sodium phosphate solution. Digestion buffer was added to each sample of two pellets prior to digestion at 65°C for 16 hours. Cartilage matrix accumulation was measured using the 1,9-dimethylmethylene blue (DMMB) assay as previously described[21]. Samples were run in triplicate in a clear flat bottom 96 well plate with DMMB dye and read at wavelengths 525nm and 595nm. Matrix production was normalized by DNA content as determined using the PicoGreen assay (Thermo Fisher). Diluted samples and λ DNA standards were run in triplicate in a black flat bottom 96 well plate with PicoGreen-Tris solution and read at excitation wavelengths 498nm and emission wavelength 528nm.

3.2.4 Histological analysis

Pellets were washed twice with PBS and fixed with 10% neutral buffered formalin at room temperature for 30 minutes. Fixed pellets were washed with PBS followed by 70% ethanol. Pellets were dehydrated with an ethanol-xylene series prior to paraffin embedding and sectioning. Sections were stained with Alcian Blue (1% in 3% Acetic Acid, Poly Scientific) and counterstained with Nuclear Fast Red (Electron Microscopy Sciences) to evaluate proteoglycan accumulation. For immunofluorescence, sections underwent antigen retrieval (BD Pharmingen) and blocking prior to primary antibodies incubation for aggrecan (1:500 dilution in 10% Goat serum in 0.1% TBS-TX100), collagen type II (1:100), collagen type X (1:100), RUNX2 (1:100), or MMP13 (1:200) (Abclonal) overnight at 4°C. Histological slides were incubated with secondary antibodies

for 1 hour at room temperature and then counterstained with DAPI (Life Technologies) for 5 minutes at room temperature.

3.2.5 Gene Expression

Analysis of gene expression was performed as previously described[49]. Briefly, total RNA of pellets was isolated using TRI Reagent RT (Molecular Research Center). cDNA was synthesized using High-Capacity cDNA Reverse Transcription Kit (Life Technologies) and amplified using SYBR Green PCR Master Mix (Life Technologies) on Applied Biosystems 7500 Fast well plates. The mean cycle threshold of housekeeping genes *GUS* and *TBP* (Ct_{hk}) was used to determine the fold change of gene expression levels compared to day 0 samples using the $\Delta\Delta C_T$ method. Relative expression levels were calculated as $x = 2^{-\Delta\Delta C_T}$, where $\Delta\Delta C_T = \Delta T - \Delta C$, $\Delta T = (Ct_{exp} - Ct_{hk})_t$, and $\Delta C = (Ct_{exp} - Ct_{hk})_{t0}$.

Table 3-1. Primer sequences for qPCR gene expression analysis.

Gene	Forward	Reverse
ACAN	GGAGTGGATCGTGACCCAAG	AGTAGGAAGGATCCCTGGCA
COL2A1	CTCCAATGGCAACCCTGGAC	CAGAGGGACCGTCATCTCCA
RUNX2	CCGGAATGCCTCTGCTGTTA	AGCTTCTGTCTGTGCCTTCTGG
COL10A1	GAACTCCCAGCACGCAGAATC	TGTTGGGTAGTGGGCCTTTT
TBP	GTGGGGAGCTGTGATGTGAA	TGCTCTGACTTTAGCACCTGT
GUS	GACTGAACAGTCACCGACGA	ACTTGGCTACTGAGTGGGGA

3.2.6 Mechanical Compression testing

At day 70 and 141, hydrogel samples were taken for stress relaxation testing. Hydrogels underwent stress relaxation with a 10% strain rate with a 500 second relaxation period while submerged in room temperature PBS. The equilibrium modulus was determined when the stress levels reached constant stress levels for 20 seconds. The Young's modulus was calculated from the linear portion of the ramp-up phase.

3.3 Results

Luciferase activity shows that the 3-cis shRUNX2 gene circuit suppresses RUNX2 activity to a greater extent than the 1-cis shRUNX2 gene circuit, as we have previously shown[49]. We observed a peak at day 14, where the suppression levels of the 1-cis and 3-cis gene circuits were 77.6% and 82.5%, respectively. At day 39 low RUNX2 suppression decreased RUNX2 activity by 53.9% and high RUNX2 suppression decreased RUNX2 activity by 74.7%. By day 48, RUNX2 activity decreases and remains low through day 70 (Fig. 3-1a). These results confirm that RUNX2 activity and the gene circuit are active throughout long- term culture.

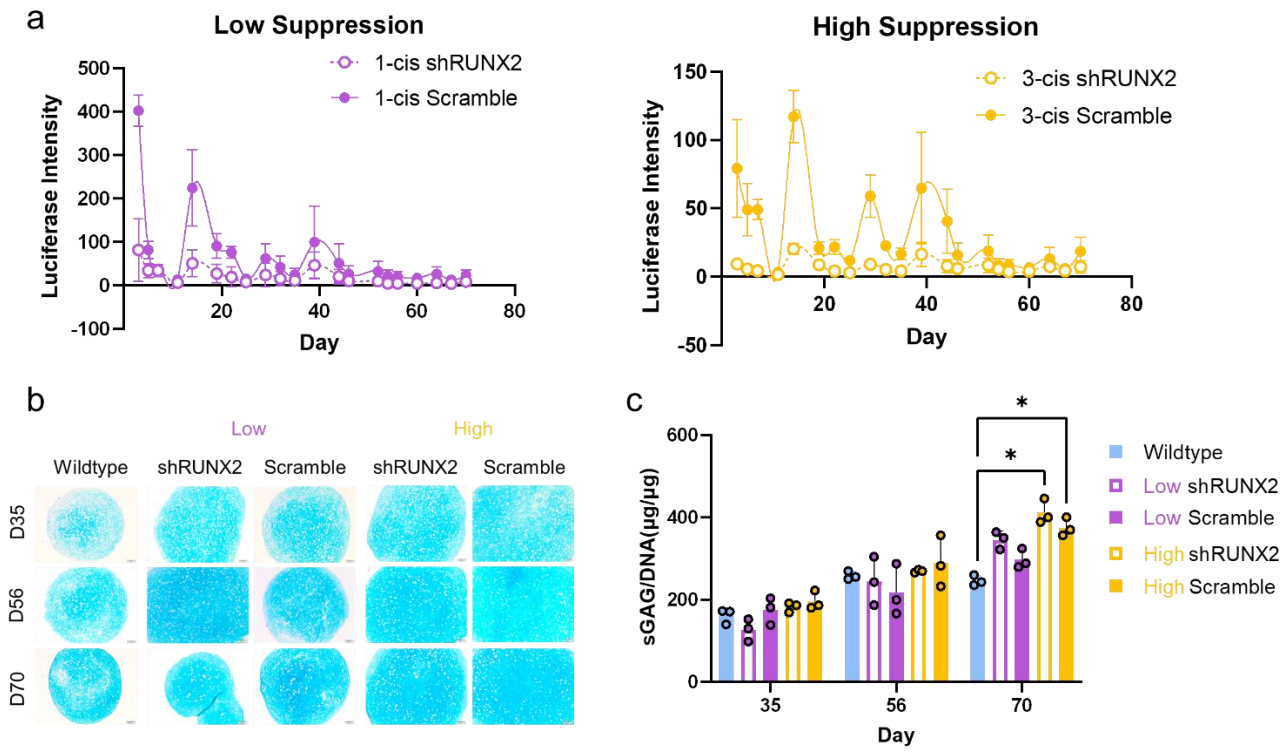

Figure 3-1. Activity of shRUNX2 gene circuit and its effect on cartilage matrix accumulation. (a) Relative RUNX2 activity of shRUNX2 gene circuit and scramble control over 70 days of chondrogenesis. (b) Alcian blue staining of histological sections of pellets at days 35, 56, and 70 of chondrogenic culture. (c) sGAG accumulation determined by DMMB assay shows increased matrix accumulation with 3-cis circuit and scramble gene circuits by day 70 (* indicates p-value < 0.05)

The benefits of increased cartilage matrix accumulation are most evident at day 70 of chondrogenic culture. Alcian blue staining shows deep rich staining across all treatment conditions

at day 35 but is most abundant at day 70 of chondrogenic culture (Fig. 3-1b). This is further confirmed using DMMB analysis. ECM accumulation was similar in all groups on days 35 and 56; however, by day 70, the genetically modified cells had more matrix accumulation, with the 3-cis gene circuit accumulating 67.2% more matrix and the 3-cis scramble accumulating 52.6% more matrix than day 70 wildtypes (Fig. 3-1c) indicating that the effects of the gene circuit are most beneficial during long-term culture.

Gene and protein expression was analyzed at different time points for chondrogenic markers, *COL2A1* and *ACAN*. At day 35, aggrecan gene expression exhibited and 7.56-fold and 8.06-fold increase with the 1-cis and 3-cis gene circuit MdChs compared to wildtype MdChs (Fig. 3-2a). This increase in aggrecan expression was sustained for 70 days of chondrogenic culture. Similarly, at day 35, the 1-cis scramble and 3-cis scramble exhibited a 3.39-fold and 4.5-fold increase, respectively (Fig. 3-2a). Aggrecan protein expression exhibited a similar trend where the gene circuit and scramble MdChs had higher expression compared to wildtype MdChs at all time-points (Fig. 3-2b). At day 35, wildtype MdChs had more collagen type II expression than the 1-cis circuit, 1-cis scramble, and 3-cis scramble (Fig. 3-2c). However, beginning at day 56, all genetically modified MdChs observe over a 2-fold increase in collagen type II gene expression compared to wildtype MdChs (Fig. 3-2c). Collagen type II immunofluorescence demonstrated an increase from days 35 to day 70 for all treatment conditions, except for 1-cis scramble MdChs (Fig. 3-2d). This further confirms the ability of the gene circuit to stabilize the chondrogenic phenotype of MdChs and indicates that the gene circuit is more effective during long-term culture.

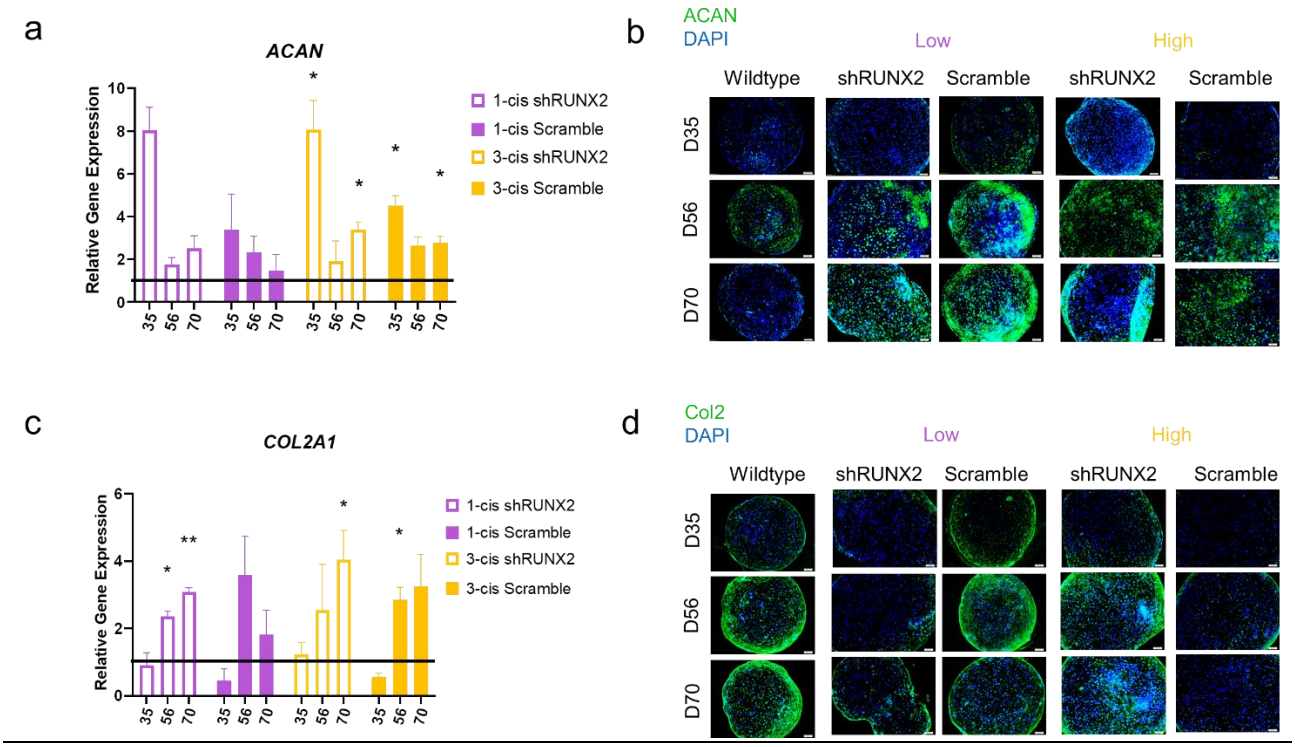

Figure 3-2. Chondrogenic gene and immunofluorescence intensity of low sensitivity and high sensitivity gene circuits at day 35, 56, and 70 normalized to wildtype MSCs. (a) ACAN gene expression of genetically modified cells are elevated compared to wildtype (* indicates p-value < 0.05 compared to wildtype MdChs) (b) ACAN immunofluorescence to demonstrate protein expression. (c) COL2A1 gene expression is elevated by day 56 of chondrogenic culture (* indicates p-value < 0.05 and ** indicates p-value < 0.005 compared to wildtype MdChs). (d) Collagen type II immunofluorescence intensity increases with chondrogenic culture.

Notably, *RUNX2* gene expression for genetically modified MdChs was lower than wildtype MdChs at all time-points beginning at day 35 and was sustained throughout the 70-day chondrogenic culture (Fig. 3-3a). RUNX2 immunofluorescence further confirms the decrease in RUNX2 with the gene circuits and scramble MdChs throughout the chondrogenic culture while RUNX2 expression in wildtype MdChs is sustained (Fig. 3-3b). Collagen type X expression was also lower for genetically modified MdChs compared to wildtype MdChs at all time points (Fig. 3-3c, d).

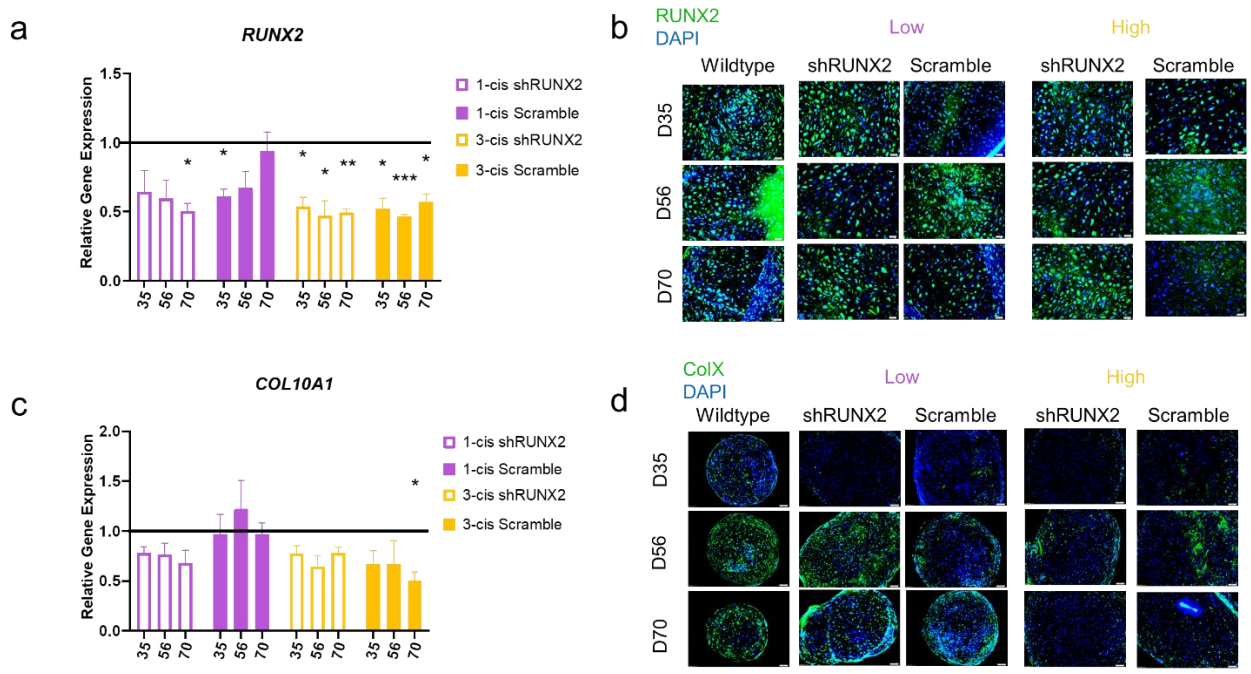

Figure 3-3. Hypertrophic gene and immunofluorescence intensity of low sensitivity and high sensitivity gene circuits at day 35, 56, and 70 normalized to wildtype MSCs. (a) RUNX2 gene expression (* indicates p-value < 0.05, ** indicates p-value < 0.005, *** indicates p-value < 0.0001) and (b) immunofluorescence shows decreased RUNX2 expression with genetically modified MdChs compared to wildtype. (c) COL10A1 gene expression (* indicates p-value = 0.030) and (d) immunofluorescence intensity shows decreased COLX expression with genetically modified MdChs compared to wildtype.

Cartilage matrix accumulation within agarose hydrogels shows a similar trend to scaffold-free pellet culture. RUNX2 suppression increases sGAG accumulation as determined by DMMB and Alcian blue staining over the 141-day chondrogenic culture (Fig. 3-4a, b). The 3-cis shRUNX2 gene circuit had 102.4% more matrix accumulation than wildtypes at day 70 and 208.9% more matrix than wildtypes at day 141. Additionally, immunofluorescence confirmed that RUNX2 expression was continuously suppressed throughout the chondrogenic culture with the 3-cis gene circuit (Fig. 3-4c). Mechanics of the constructs showed that the shRUNX2 gene circuit increased the Young's modulus at day 70 compared to wildtype, but this increase was not sustained (Fig. 4d). The equilibrium modulus for shRUNX2 at both day 70 (4.9 kPa) and day 141 (9.0 kPa) was stiffer than wildtype (1.68 kPa and 6.67 kPa, respectively) (Fig. 3-4e).

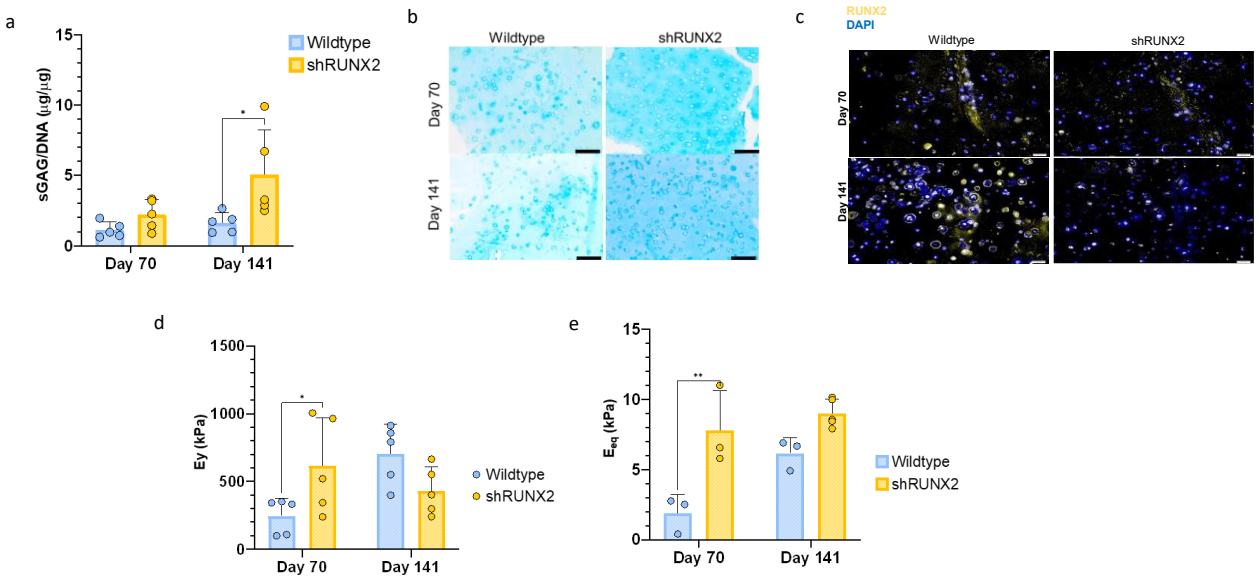

Figure 3-4. Response of genetically engineered MdChs in agarose hydrogels at day 70 and 141.(a) sGAG quantification of hydrogels normalized by DNA shows increased cartilage matrix accumulation (* indicates p-value = 0.014). (b) Alcian blue staining shows abundant matrix content. (c) RUNX2 immunofluorescence confirms decreased RUNX2 protein intensity with RUNX2 suppression. (d) Young's modulus of genetically modified cellular hydrogels was stiffer by day 70 but was lower by day 141 (* indicates p-value = 0.002). (e) The equilibrium modulus of genetically modified cellular hydrogels increased throughout culture (** indicates p-value 0.049).

3.4 Discussion

This study shows the long-term viability of cell- autonomous RUNX2 suppression during MdCh neo-cartilage formation and its effects on cartilage matrix accumulation. The RUNX2 gene circuit sustained suppressed RUNX2 activity throughout the 70-day chondrogenic culture while also improving the expression of chondrogenic genes and cartilage matrix accumulation compared to wildtype MdChs long-term. Long-term functionality of the gene circuit is confirmed through the sustained decrease in RUNX2 expression throughout culture. While gene circuit- regulated RUNX2 activity did not significantly increase cartilage matrix production during early-stage chondrogenesis, significant changes were observed by day 70. The reduction of cartilage matrix accumulation observed with wildtype MdCh coincides with the loss of cartilage matrix found in other long-term chondrogenic studies and is potentially due to the upregulation of metalloproteinase expression[20,77–80]. This is further validated in this study where we observe an

increase in MMP13 expression by day 70 of wildtype MdChs. The increased levels of cartilage matrix accumulation by genetically modified MdChs are potentially due to the decrease in MMP13 and other hypertrophic factors, such as ColX and RUNX2. Overall, this indicates that the gene circuit improves cartilage matrix accumulation, and these benefits are sustained over time.

Similar to the scaffold-free system, we observed an increase in cartilage matrix accumulation by genetically modified RUNX2- suppressed MdChs. Stress relaxation testing showed that this increase in sGAG accumulation correlated with increased equilibrium stiffness of neo-cartilage constructs. At day 70, the Young's modulus and equilibrium modulus are higher for the RUNX2-suppressed gene circuit neo-cartilage constructs than the wildtypes, which coincides with the sGAG quantification. The equilibrium modulus increases with cartilage sGAG by day 141. Similarly, Hu et al and Farrell et al observed a strong positive correlation between GAG content and the equilibrium modulus[18,20]. However, in the Farrell et al study the GAG and equilibrium modulus of MdCh constructs decrease by day 112 of chondrogenesis. We observed a decrease in Young's modulus for the genetically modified constructs at day 141 are contrary to the sGAG data. This could potentially be due to the cleavage of sGAG chains within the neo-cartilage constructs that were trapped within the constructs, which would also account for the slight increase in the equilibrium modulus. To confirm these results, we must isolate and quantify the non-degraded sGAG chains. Additionally, cartilage is composed of both collagen and aggrecan; therefore, simply evaluating sGAG content is insufficient to determine cartilage quality. The hydroxyproline assay should be used to quantify collagen content of the neo-cartilage constructs to assess whether neo-cartilage mechanics are related to the ratio of collagen and aggrecan content.

Our findings show that long-term suppression of RUNX2 improves cartilage matrix accumulation of MdChs, but RUNX2 suppression of MdChs alone does not create neo-cartilage

that has mechanical properties sufficient to restore cartilage function. Based on the mechanics of cartilage, an increase in sGAG accumulation should result in increased stiffness of cartilage constructs[18]. Although we observed an overall increase in cartilage matrix production within neo-cartilage constructs, the mechanics of the constructs are not similar to articular cartilage, which is typically within the range of 0.5 to 0.9MPa[81]. Additional long-term experiments could provide insights to the mechanisms and timeframe of MdCh cartilage regeneration and degradation. Studies to 140 days of chondrogenic culture could further amplify the observed differences in these studies and could elucidate whether the sustained cartilage matrix is due to the downregulation of matrix metalloproteinases, the upregulation of aggrecan expression, or a combinatorial response of the two. This indicates that while we demonstrated improvements in the stabilization of the chondrogenic phenotype of MdChs and increased matrix retention of our engineered tissue, further work must be completed to increase cartilage matrix content and replicate cartilage organization. For example, the use of dynamic loading, hypoxic conditions, and treatment with inorganic phosphate (Pi) have been shown to improve cartilage matrix outcomes in chondrogenic models[20,46,82,83]. Utilizing these methods in conjunction with the shRUNX2 gene circuit could further increase cartilage matrix accumulation of MdChs to become more physiologically relevant for cartilage defect repair.

CHAPTER 4 : Combinatorial Effect of Phosphate Treatment and RUNX2 Suppression to Improve Mesenchymal Stem Cell-Derived Cartilage Regeneration

4.1 Introduction

Mesenchymal stem cells (MSCs) are a promising cell source for cartilage repair because of their ability to undergo chondrogenesis[25,30]. However, MSCs used during cartilage tissue engineering are limited by their unstable chondrogenic phenotype[20]. After chondrogenic induction, MSC-derived chondrocytes (MdChs) continue down the endochondral ossification pathway and begin to express hypertrophic markers both *in vitro* and *in vivo*[84]. a multitude of factors can drive MdChs down the endochondral ossification pathway, including hypertrophic growth factors, inflammation, and calcium phosphate microcrystals in the joint[26,52,63,84].

Osteoarthritis (OA) and cartilage injuries can lead to an activated joint, defined by the elevation of calcification and/or inflammatory factors. For example, these joints also have elevated levels of calcium phosphate Ca×Pi complexes, such as basic calcium phosphate crystals (BCP), hydroxyapatite, or calcium pyrophosphate crystals[47]. The levels increase during osteoarthritis and cartilage injury due to the rise of ALP which cleaves pyrophosphate (PPi) to produce inorganic phosphate (Pi) release into the joint[47]. The presence of Ca×Pi has been linked to increased production of MMP3 and MMP13 in hypertrophic chondrocytes, metalloproteinases known to degrade cartilage matrix[48]. MdChs used to treat cartilage injuries within these activated joints are hence subjected to factors that have been shown to lead to hypertrophy and a reduction in articular

cartilage extracellular matrix production[52]. Indeed, Pi levels that are found in advanced OA, has extensively been shown to induce hypertrophy MdChs[46,61,63,85].

In Chapter 2, we observed that continuous Pi treatment increased cartilage extracellular matrix (ECM) accumulation, but also increased expression of MMP13 and collagen type X, the quintessential marker of hypertrophy, and mineralization. Therefore, to utilize Pi to improve cartilage matrix accumulation, it is imperative to inhibit Pi-induced hypertrophy of MdChs. Within chapter 3 and Wu et al, our lab has previously shown that the use of a gene circuit designed to induce cell-autonomous and scalable RUNX2 suppression successfully reduced RUNX2, ColX, and MMP13 expression. Within this study, we investigated the relationship between Pi and RUNX2 using two approaches. First, we evaluated the combined effects of Pi treatment and RUNX2 suppression to inhibit hypertrophic differentiation and decrease mineralization. Second, we evaluated whether priming cells with low levels of Pi prior to exposure to high Pi levels would enhance chondrogenesis and decrease mineralization. We hypothesize that the pre-treatment of Pi will increase cartilage matrix accumulation and prepare the tissue for the highly phosphorus environment that the cells will be subjected to *in vivo* and that RUNX2 suppression would reduce Pi-induced mineralization.

4. 2 Methods

4.2.1 Cell Culture

4.2.1.1 Cell Expansion

Bone marrow-derived MSCs were gifted by Dr. Rodrigo Somoza in collaboration with CWRU Center for Multimodal Evaluation of Engineered Cartilage (CMMEC, Cleveland, Ohio). Cells were initially seeded at a density of 4,000 cells/cm^2. MSCs were expanded in monolayer in expansion media (Low glucose Dulbecco's modified Eagle's medium (DMEM) (Invitrogen), 10%

Fetal Bovine Serum (Invitrogen), 1% Antibiotic-Antimycotic (Invitrogen), and 10ng/ml Fibroblast Growth Factor (FGF) (Shenandoah). At 80% confluency, cells were lifted using 0.25% Trypsin-EDTA (Invitrogen) and neutralized using a solution composed of 10% Fetal Bovine Serum (Invitrogen) and 90% low glucose DMEM (Invitrogen). Cells were replated at a seeding density of 4,000 cells/cm^2 until a population doubling of 11 is reached.

4.2.1.3 Chondrogenic Differentiation and Phosphate Treatment

To create cell pellets, $2.5x10^5$ cells suspended in chondrogenic media were placed in each well of a U bottom 96 well plates (ThermoFisher) and centrifuged at 1640 RPM for 5 minutes. Pellets were cultured in chondrogenic media at 37°C at 5% CO_2. Chondrogenic pellet culture medium consisted of high glucose Dulbecco's Modified Eagles Medium (Gibco), 1% ITS+ Premix (Corning), 1% Non- essential amino acids (Gibco), 1% antibiotic-antimycotic (Invitrogen), 40µg/ml L-proline (Sigma), 50 µg/ml ascorbic acid 2- phosphate (Sigma), 0.1µM dexamethasone (Sigma), and 10ng/ml TGF-β1 (Shenandoah)[62]. Pi treatment groups received 0, 5, or 20mM of βGP from day 0 to day 14 of chondrogenesis for Pi pre-treatment and 20mM βGP from days 14 to 28 to simulate the high Pi levels (Fig. 4-1).

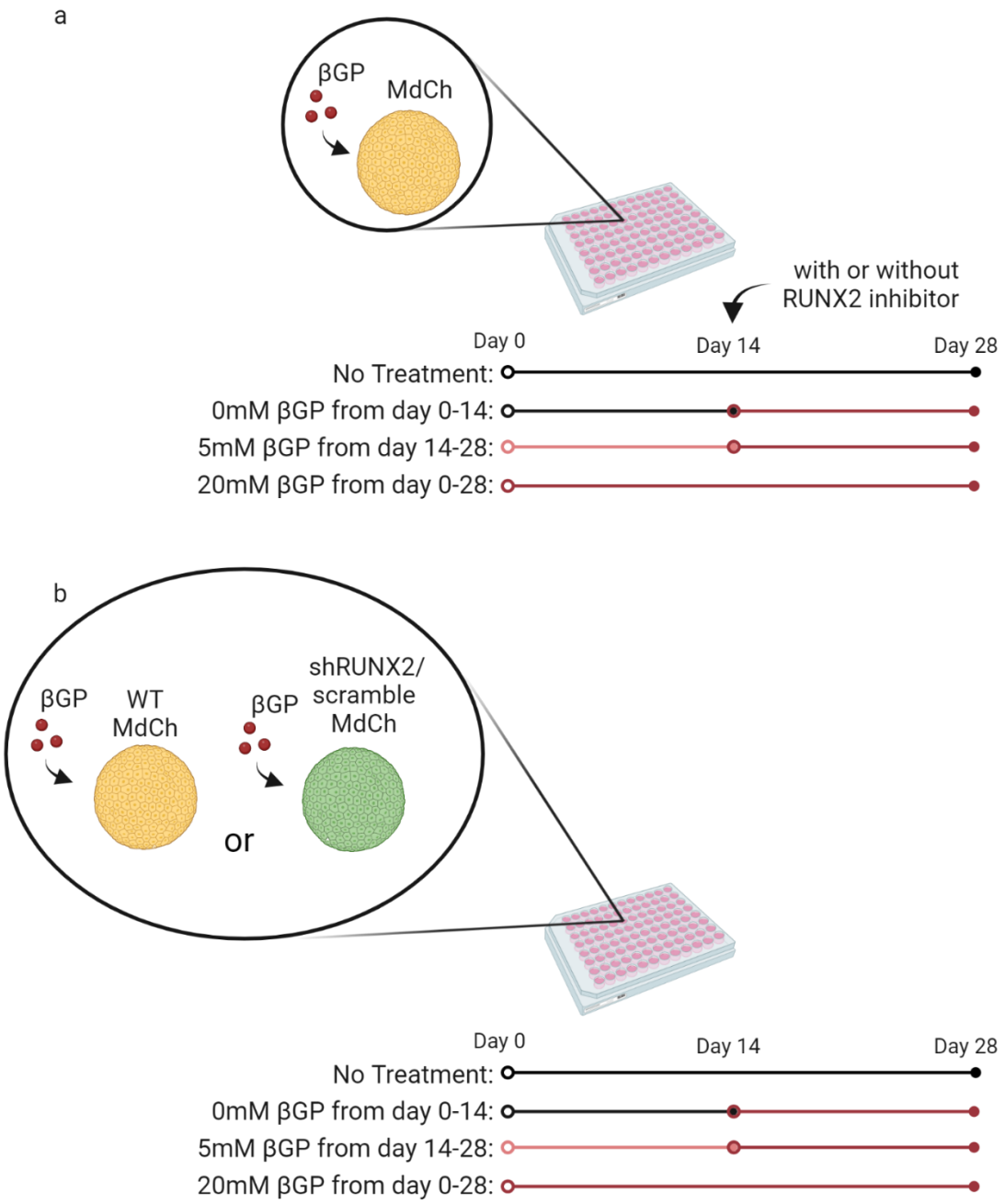

Created with BioRender.com

Figure 4-1. Experimental design. (a) MdCh pellets were treated with 0, 5, or 20mM of βGP from days 0-14. All pellets except for WT controls received 20mM βGP starting at day 14. At day 14, a RUNX2 inhibitor was introduced to the chondrogenic culture. (b) MdChs reprogrammed with the RUNX2-supressing or scrambled gene circuits and wildtype (WT) MdChs were treated with 0, 5, or 20mM of βGP from days 0-14. All pellets except for non-treated controls received 20mM βGP beginning at day 14.

4.2.1.2 RUNX2 suppression

Two methods were used to induce RUNX2 suppression.

4.2.1.2.1 RUNX2 Inhibitor

Based on previous data, such as the luciferase activity outlined in Chapter 3, there is upregulation of RUNX2 activity at day 14 of chondrogenesis. Beginning at day 14 of chondrogenic culture, wildtype MdChs were treated with 1μM RUNX2 inhibitor (Selleck Chem) to inhibit RUNX2 activity.

4.2.1.2.2 Auto-Regulated RUNX2 Suppression

Cells were transduced with our previously developed auto-regulatory gene circuit that suppresses RUNX2 levels by 80% (Fig. 4-2)[76]. Cells were plated at a seeding density of 10,000 cm^2 and were exposed to the lentiviral supernatant (MOI of 5) with polybrene in the absence of antibiotics for 24 hours[49]. After lentiviral was removed, cells were washed with PBS. Transduced cells were selected using 1μg/ml puromycin (Sigma) and expanded in monolayer before being seeded into pellet culture. Fig. 4-2)

Figure 4-2. Schematic of gene circuit.

4.2.2 Luciferase Assay

Luciferase activity of pellets was measured in 96 well plates at every media change. Chondrogenic media was replenished six hours prior to luciferase measurement. Thirty minutes prior to measurement, D-Luciferin (Biovision) was added to culture media and incubated at 37°C.

Luminescence was measured using the SYNERGY H1 microplate reader (BioTek). Culture media was changed after luciferase readings.

4.2.3 Biochemical Analysis

Pellets were harvested on days 14 and 28 of chondrogenic culture and digested using a 0.3 units/ml papain in a cysteine, EDTA, and sodium phosphate buffer. Samples were incubated in the solution at 65°C for 16 hours. Cartilage matrix accumulation was measured using the 1,9-dimethylmethylene blue (DMMB) assay as previously described[21]. Samples and chondroitin sulfate standards were diluted in papain buffer. Samples were run in triplicate in a clear flat bottom 96 well plate with DMMB dye and read at wavelengths 525nm and 595nm. Matrix production was normalized by DNA content as determined using the PicoGreen assay (Thermo Fisher). Diluted samples and λ DNA standards were run in triplicate in a black flat bottom 96 well plate with PicoGreen-Tris solution and read at excitation wavelengths 498nm and emission wavelength 528nm.

4.2.4 Histological analysis

Pellets were washed twice with PBS and fixed with neutral buffered formalin at room temperature for 30 minutes. Fixed pellets were washed with PBS followed by 70% ethanol. Pellets were dehydrated with an ethanol series prior to paraffin embedding and sectioning. Sections were stained with Alcian Blue (1% in 3% Acetic Acid, Poly Scientific) and counterstained with Nuclear Fast Red (Electron Microscopy Sciences) to evaluate proteoglycan accumulation. Calcium deposition was visualized using a 2% Alizarin Red S dye (pH 4.3, Sigma). For immunofluorescence, sections underwent antigen retrieval (BD Pharmingen) and blocking prior to incubation with primary antibodies (Abclonal) overnight at 4°C. Each antibody was diluted in 10% goat serum in 0.1% TBS-TX100 at the following concentrations: aggrecan (1:500 dilution in

10% Goat serum in 0.1% TBS-TX100), collagen type II (1:100), collagen type X (1:100), RUNX2 (1:100), or MMP13 (1:200). Histological slides were incubated with secondary antibodies for 1 hour at room temperature. Sections were counterstained with DAPI (Life Technologies) for 5 minutes at room temperature to visualize the cell nuclei.

4.2.5 Gene Expression

Analysis of gene expression was performed as previously described[49]. Briefly, total RNA of pellets was isolated using TRI Reagent RT (Molecular Research Center). cDNA was synthesized using High-Capacity cDNA Reverse Transcription Kit (Life Technologies) and amplified using SYBR Green PCR Master Mix (Life Technologies) on Applied Biosystems 7500 Fast well plates. The mean cycle threshold of housekeeping genes *GUS* and *TBP* (Ct_{hk}) was used to determine the fold change of gene expression levels compared to day 0 samples using the $\Delta\Delta C_T$ method. Relative expression levels were calculated as $x = 2^{-\Delta\Delta C_T}$, where $\Delta\Delta C_T = \Delta T - \Delta C$, $\Delta T = (Ct_{exp} - Ct_{hk})_t$, and $\Delta C = (Ct_{exp} - Ct_{hk})_{t0}$.

Table 4-1. Primer sequences for qPCR gene expression analysis.

Gene	Forward	Reverse
ACAN	GGAGTGGATCGTGACCCAAG	AGTAGGAAGGATCCCTGGCA
COL2A1	CTCCAATGGCAACCCTGGAC	CAGAGGGACCGTCATCTCCA
COL10A1	GAACTCCCAGCACGCAGAATC	TGTTGGGTAGTGGGCCTTTT
MMP13	TTGCAGAGCGCTACCTGAGA	CCCCGCATCTTGGCTTTTTC
TBP	GTGGGGAGCTGTGATGTGAA	TGCTCTGACTTTAGCACCTGT
GUS	GACTGAACAGTCACCGACGA	ACTTGGCTACTGAGTGGGGA

4.3 Results

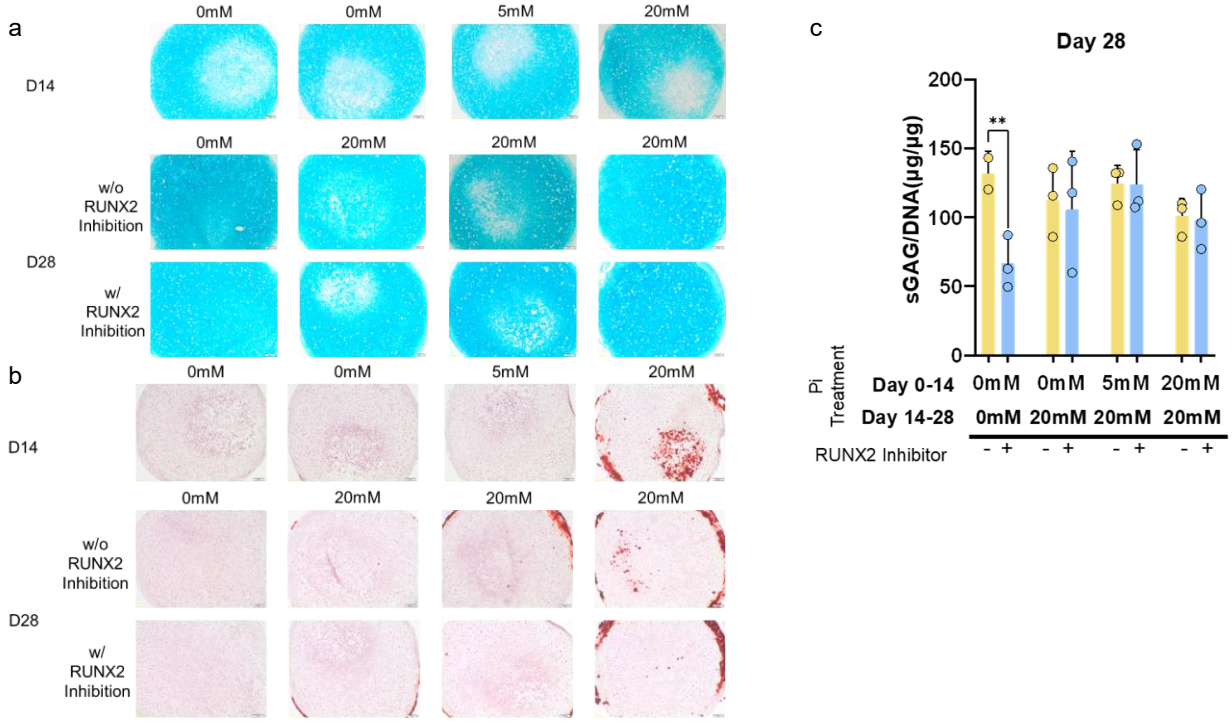

Figure 4-3. RUNX2 inhibition did not increase cartilage ECM and reduced mineralization. (a) Rich Alcian blue staining showed abundance of cartilage matrix was produced in all groups. (b) Alizarin red staining demonstrated RUNX2 inhibition reduced mineralization. (c) sGAG quantification shows a decrease in cartilage matrix of MdChs with RUNX2 inhibition and no Pi treatment (** indicates p-value = 0.008).

First, we evaluated cartilage ECM accumulation by MdChs in response to the RUNX2 inhibitor. At day 28 of chondrogenesis, we observed abundant matrix accumulation as shown by Alcian blue staining throughout all treatments (Fig. 4-3a). Additionally, there were no significant changes in ECM production pellets treated with the RUNX2 inhibitor versus untreated (Fig. 4-3c). However, RUNX2 inhibition without Pi treatment decreased sGAG quantity ($p < 0.008$). Alizarin red staining showed that RUNX2 inhibition successfully decreased mineralization of Pi treated pellets.

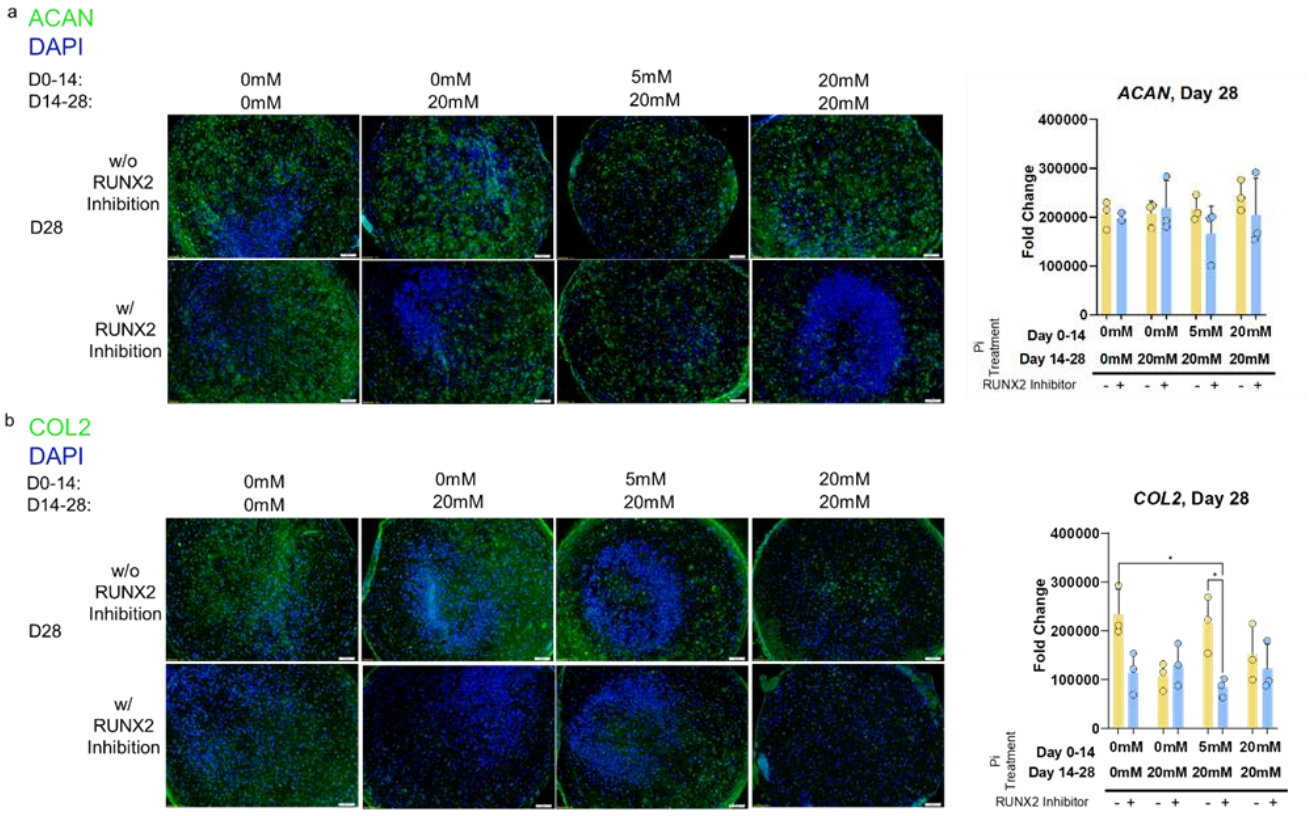

Figure 4-4. Chondrogenic expression of MdChs with Pi treatment and delayed RUNX2 inhibition. RUNX2 inhibition did not alter (a) aggrecan expression but decreased (b) collagen type II expression (* indicates $p < 0.05$).

Immunofluorescence confirmed that the inhibitor reduced RUNX2 protein expression (Fig. 4-5a). Additionally, immunofluorescence and gene expression showed that collagen type II expression decreased with RUNX2 inhibition, but there was no effect on aggrecan expression (Fig. 4-4a, b). RUNX2 inhibition had no effect on the collagen type X expression and had a mixed effect on MMP13 expression (Fig. 4-5b, c).

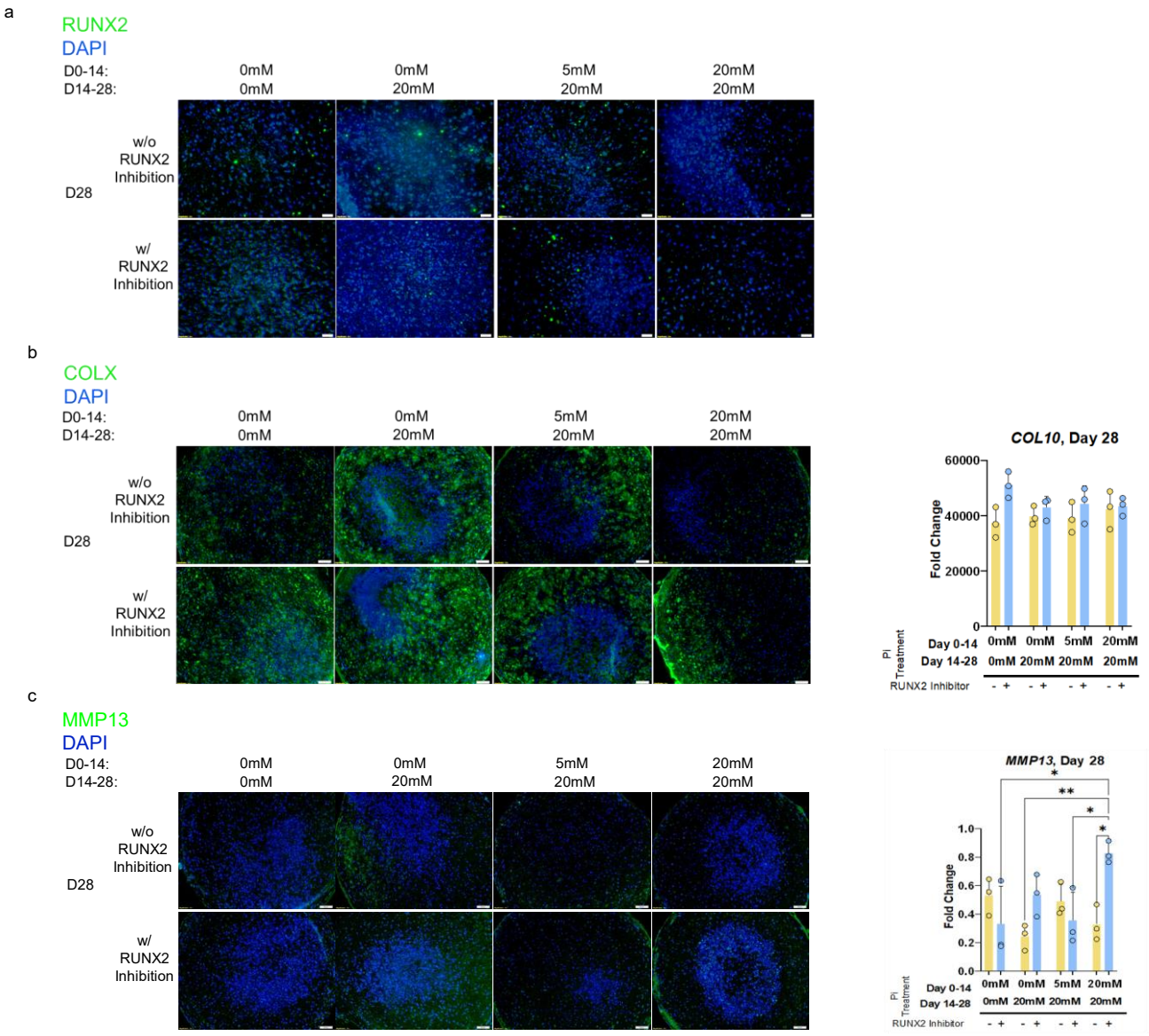

Figure 4-5. Hypertrophic expression of MdChs with Pi treatment and delayed RUNX2 inhibition. (a) RUNX2 inhibition was confirmed with immunofluorescence. RUNX2 inhibition did not decrease (b) collagen type X expression or (d) MMP13 expression (* indicates $p < 0.05$, ** indicates $p < 0.01$).

We next utilized our cell-regulated RUNX2 gene circuit to evaluate the effects of Pi on MdCh chondrogenesis and hypertrophy. Interestingly, Pi treatment lowered RUNX2 activity in the scramble control pellets (Fig. 4-6a). In the previous experiments, we observed no significant increase in cartilage matrix accumulation with combined RUNX2 inhibition and Pi treatment. With the gene circuit, Alcian blue staining shows that the gene circuit has the most abundant matrix but

does not vary significantly in conjunction with Pi treatment (Fig. 4-6c). The most notable difference is that the shRUNX2 gene circuit reduced mineralization with Pi treatment (Fig. 4-6d). In particular, the low Pi primed gene circuit pellets had no mineralization by day 28, while both wildtype and scrambled controls underwent mineralization (Fig. 4-6d).

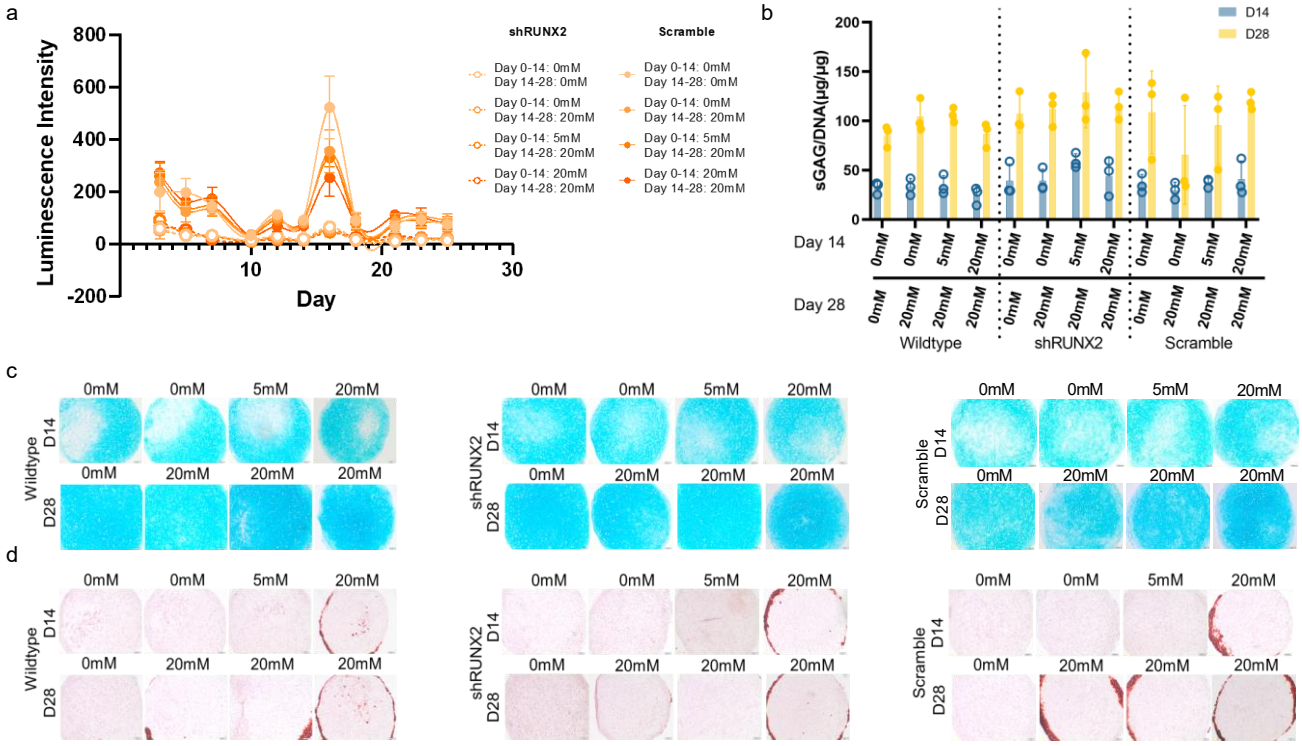

Figure 4-6. Pi treatment and RUNX2 suppression increases matrix production and decreases mineralization. (a) Luciferase activity shows RUNX2 activity decreases with Pi treatment. (b) sGAG quantification through DMMB shows slightly elevated quantification with RUNX2 suppression, especially when primed with 5mM βGP. RUNX2Cartilage matrix and accumulation. (c) Alcian blue showed more abundant staining with RUNX2 suppression and (d) Alizarin red showed decreased mineralization with RUNX2 suppression.

4.4 Discussion

In Chapter 2, we saw that Pi treatment had the potential to increase MdCh matrix production, but also accelerated their hypertrophic differentiation, which agrees with our previous work[46]. Here, we show that cell-regulated RUNX2 suppression as a co-treatment abrogates premature hypertrophy of MdChs while permitting enhanced matrix accumulation to occur. Specifically, we found that priming with low levels of Pi abundance, as defined in Chapter 3, had

the greatest effect in resisting hypertrophic changes as indicated in decreased expression gene and protein markers.

Chemical RUNX2 inhibition with Pi treatment alone did not improve cartilage matrix accumulation of MdChs, but reduced Pi-induced mineralization. Interestingly, wildtype MdChs treated with the RUNX2 inhibitor reduced the amount of accumulated sGAG. This is likely an indicator that high RUNX2 inhibition is detrimental to cartilage matrix accumulation and should not be constitutively suppressed, a finding in line with Wu et. al[49]. However, it appears that treatment with Pi rescued the matrix loss. Additionally, collagen type II gene expression decreased with exposure to high Pi. While there is no increase in cartilage matrix, the fact that collagen type II does not change when primed with low Pi prior to high Pi shows that Pi priming benefits matrix retention.

The complex dosage and timing required for the RUNX2 inhibitor led us to utilize our RUNX2-suppressing gene circuit to regulate RUNX2 activity. Our data shows that MdChs not treated with Pi have higher RUNX2 activity while high Pi treatment decreased RUNX2 activity. This is contradictory to our hypothesized pattern of RUNX2 activity, suggesting that the regulatory pathway activated by Pi is not solely RUNX2 dependent and might work through alternative signaling pathways. Literature shows that Pi upregulates the Raf/MEK/ERK pathway which have been known to regulate chondrocyte differentiation and collagen production[64,86,87]. Additionally, Rui et al. has shown that Pi promotes osteogenic differentiation by upregulating the non-canonical Wnt pathway in hMSCs[88]. Cell-regulated RUNX2 suppression consistently decreased mineralization across MdChs treated with Pi, unlike wildtype and scramble MdCh controls. Together, these results suggest that Pi treatment alone is not sufficient to significantly increase cartilage matrix accumulation. However, the most important finding is that RUNX2 inhibition

reduced Pi-induced hypertrophy and mineralization. Pi is often used to induce hypertrophy in MdChs and is upregulated with the presence of BCP crystals during varying stages of osteoarthritis[47,48,63,89]. The response of MdChs due to Ca×Pi exposure has been shown to increase ColX, MMP13, MMP3, but few studies have explored how to mitigate this shift from a chondrogenic state to a hypertrophic state in the presence of Ca×Pi [39,48,90]. Therefore, our findings suggest that MdChs with the cell-autonomous gene circuit would be better suited for cartilage tissue repair within an activated joint.

While we have confirmed that RUNX2 suppression can reduce Pi-induced mineralization and matrix loss; we ultimately still need to further increase cartilage matrix accumulation to improve cartilage tissue engineering outcomes for defects. Within Chapter 3, we determined that the most significant effects of the gene circuit are experienced at later timepoints; therefore, further evaluation of Pi treatment during neo-tissue formation long-term might elucidate the turnover of cartilage matrix accumulation and have more significant effects to increase neo-cartilage stiffness, could potentially reduce incidence of post-traumatic osteoarthritis after cartilage injury.

CHAPTER 5 : Conclusions and Future Directions

Mesenchymal stem cells (MSC) are a promising cell source for cartilage tissue engineering due to their multipotentiality and abundance within the body, despite their unstable chondrogenic phenotype. The unstable chondrogenic phenotype of MSC-derived chondrocytes (MdChs) leads to loss of cartilage extracellular matrix (ECM), resulting in non-functional cartilage. The overarching goal of this dissertation was to investigate cell-based methodologies in MdChs to improve cartilage matrix accumulation for cartilage defect repair. The first approach was to evaluate the cell-state response of MdChs during chondrogenesis when exposed to varying concentrations of inorganic phosphate (Pi). Next, we evaluated the long-term effects of our previously established cell-regulated shRUNX2 gene circuit on MdCh cartilage matrix accumulation and compressive mechanics. Lastly, we investigated whether the combinatorial treatment of these two methods would result in increased cartilage matrix accumulation. Further discussion on next steps is provided in the Future Directions section.

5.1 Summary

5.1.1 Aim 1

To improve cartilage matrix deposition, we initially investigated the response of MdChs to Pi treatment. In Aim 1, MdChs were subjected to varying concentrations of βGP at early, late, or continuously through chondrogenesis to induce Pi secretion. Through this, we first observed that Pi abundance (defined by Pi concentration normalized by DNA content) was not only determined by βGP concentration but by cell state. Next, we determined that high Pi abundance, >170μg Pi/μg

DNA, increased cartilage matrix accumulation, but also increased expression of hypertrophic markers, RUNX2, ColX, and MMP13, and tissue mineralization.

The observed effects of this aim are consistent with previous literature evaluating both ATDC5 chondrogenesis as well as MdCh hypertrophy[46,61,63,88]. This study further confirms that the effect of Pi abundance is both time and dosage dependent and that there is a level of Pi abundance in which Pi becomes detrimental to MdCh cartilage accumulation. Interestingly, continuous Pi abundance increased sulfated glycosaminoglycan (sGAG) production while early low Pi abundance increased collagen type II. These results are potentially due to Pi expediting chondrogenic matrix production. While the exact mechanism responsible for these effects are not fully understood, the upregulation of these quintessential markers for chondrogenesis observed by MdChs within this aim poses an interesting question regarding priming MdCh pellets with Pi to prepare pellets for exposure to an activated high Pi environment.

5.1.2 Aim 2

A major limitation with using MdChs for cartilage tissue repair is their unstable chondrogenic phenotype. After chondrogenic induction, MdChs continue down the endochondral ossification pathway, inducing a hypertrophic shift leading to an increase in collagen type X and matrix metalloproteinases. Therefore, in Aim 2, we utilized a synthetic cell-regulated shRUNX2 gene circuit to inhibit hypertrophic differentiation while also improving the long-term stability of MdCh chondrogenic phenotype and the resultant compressive mechanics. RUNX2 activity remained active throughout a 70-day chondrogenic culture showing promise for long-term *in vivo* work. By day 70, we observed an increase in cartilage matrix accumulation with both low and high RUNX2 suppression compared to wildtype MdChs. Additionally, a decrease in hypertrophic

marker expression was observed, which coincides with the desired outcomes for cartilage tissue engineering, consistent with work published by Wu et al [49].

Cartilage constructs that underwent long-term chondrogenic culture observed an increase in sGAG quantity from day 70 to 141. Genetically modified MdChs had more sGAG by day 141 than wildtype MdChs. Additionally, when evaluating compression of cartilage constructs on days 70 and 141 of chondrogenic culture, high RUNX2 suppression increased stiffness compared to wildtype MdChs. The positive correlation between sGAG content and equilibrium modulus are findings consistent with previous findings[20,91]. However, a limitation of the findings in this study is that the stiffness of our genetically modified MdCh construct is an order of magnitude less stiff than native cartilage[2,20,81,92]. This difference in magnitude is potentially attributed to hydrogel assembly and culture conditions. MdCh chondrogenesis benefits from cell-cell contact and the heterogeneous dispersion of cells within the agarose and lack of diffusion creates clusters of decreased cartilage matrix accumulation and decreased compressive stiffness[93–95]. While genetically modified MdChs improves cartilage matrix accumulation and stiffness compared to wildtype MdChs, it is still insufficient for cartilage repair. In the context of cartilage injuries, mechanical mismatch can lead to increased mechanical stresses and develop into post-traumatic osteoarthritis (PTOA). Therefore, further work to improve the deposition of cartilage ECM must be explored prior to use for cartilage defect healing.

5.1.3 Aim 3

A challenge in using MdChs for cartilage healing is that they are exposed to a highly activated environment that induces hypertrophy and mineralization. In Chapters 2 and 3, we investigated two independent methods that increase matrix accumulation long-term: inorganic phosphate treatment and RUNX2 suppression. Therefore, in Chapter 4 we investigated the

combinatorial effects of these two methods. First, we investigated whether combined RUNX2 inhibition and Pi treatment would result in higher matrix accumulation and reduce Pi-induced hypertrophy in neo-tissues. Pi treatment decreased RUNX2 activity and RUNX2 suppression resulted in decreased mineralization of MdChs when exposed to Pi. Our findings shows that while Pi does not significantly increase cartilage matrix accumulation, the use of the RUNX2 gene circuit can be used to mitigate unwanted cartilage matrix mineralization. Second, we investigated whether Pi priming would increase cartilage matrix accumulation prior to exposure to an activated environment. Since Pi is upregulated during osteoarthritis and cartilage mineralization, priming pellets with Pi would improve engineering outcomes for cartilage defect repair exposed to an activated environment[40,47,52,96]. While our findings did not show that pellet priming significantly improved cartilage matrix accumulation, data from Chapter 3 suggests that more evident changes will be observed with longer-term culture.

5.1.4 Impact

MSC-derived cartilage tissue regeneration has the potential to revolutionize repair of cartilage defects despite the limitations of chondrogenic phenotype instability. This instability has been addressed by tailoring culture conditions to overexpress chondrogenic factors or inhibit the MdCh hypertrophic shift[49,97,98]. In this dissertation, we evaluated multiple approaches to increase cartilage matrix accumulation long-term, including Pi treatment and RUNX2 suppression.

Optimizing engineered cartilage neo-tissues to achieve native cartilage mechanics while also resisting hypertrophy-induced matrix loss has the potential to reduce incidence of PTOA. Successful increase in cartilage matrix and reduction in mineralization within an activated environment using genetically modified MdChs brings us one step closer to optimizing MdChs for treatment of cartilage defects. In this dissertation, we have shown that use of our RUNX2-

supressing gene circuit inhibits Pi-induced and time-dependent MdCh hypertrophy. The time and dose response to Pi treatment extends further than cartilage tissue engineering. The combinatorial effects are particularly applicable to osteochondral applications, where integration of cartilage, calcified cartilage, and bone is critical for repair.

Additionally, mineralization and irregular mechanics upregulates the expression of inflammatory factors such as interleukin 1 (IL-1) and interleukin 6 (IL-6) that result in cartilage tissue degradation[39,47,52,58]. While ongoing efforts in the cartilage field have investigated cartilage's response to these factors, there are insufficient studies to prevent these changes from occurring. This work provides a framework on how to protect MdCh from mineralization, mechanics, and inflammatory-associated phenotype shifts and cartilage matrix degradation.

5.2 Future Directions

5.2.1 Improving Cartilage ECM Accumulation

In this thesis, we encountered a common obstacle of increasing cartilage matrix accumulation. Hypoxia and dynamic loading are among strategies currently being investigated to improve MdCh matrix deposition to address this limitation[20,22,73,99,100]. Within the body, articular cartilage is normally subjected to both a hypoxic environment and dynamic loading due to joint movement[92]. To study hypoxic conditions, chondrocyte pellets were maintained and cultured in either hypoxic conditions (2% oxygen) or under standard conditions (20% oxygen)[101]. Hypoxia studies show that chondrocytes cultured under hypoxic conditions have higher sulfated glycosaminoglycan accumulation and collagen type II and aggrecan gene expression[22,73]. Therefore, culturing our MdChs under hypoxic conditions may increase cartilage matrix as well as prime cells for *in vivo* applications.

Dynamic mechanical loading during cartilage formation regulates the maintenance of articular cartilage[2]. Dynamic loading during chondrogenic culture increases matrix accumulation and stiffness compared to free swelling[20]. Mechanical stimuli of the cells aids in diffusion of nutrients throughout the neo-tissue and increases matrix production[18,83,102]. The addition of either of these treatment strategies, in conjunction with our current methodologies, may provide us with the needed stimulus to increase cartilage matrix accumulation to match those within the knee joint.

5.2.2 Dictating Cartilage Organization

Cartilage has a unique hierarchical structure, with four distinct layers: the superficial layer, the transitional layer, the deep layer, and the calcified layer[1,18,19,28]. Each of these layers have a structural organization of collagen and chondrocyte density[1,18]. One method to recreate the cartilage organization using scaffolds to act as a guidance for tissue formation. Scaffolds can provide extracellular biomechanical and biochemical cues that lead to MSC differentiation[103–105].While we used an agarose scaffold in this thesis, additional scaffolds for cartilage tissue engineering include fibrin, collagen type I, alginate, and polyglycolic acid (PGA)[106]. To further improve cartilage organization, electrospinning can synthesize scaffolds from continuous fibers of various materials, such as collagen, fibrin, and hyaluronic acid[107–109]. Electrospinning can tailor scaffold structure and porosity that would create a more optimal environment for cartilage regeneration and recapitulate cartilage layers[107,109].

5.2.3 Evaluate Cartilage Regeneration In vivo

To assess the properties of cartilage neo-tissue regeneration and retention more accurately, *in vivo* studies should be performed. Rodent defect models provide the complex immunological systems and regulatory pathways that are present during cartilage injury and repair[110–112]. In these studies, a 2mm diameter critical size defect is made to the cartilage in the femoral head and filled

with cells[112]. *In vivo* evaluation of cartilage healing could be assessed using MRI[113,114]. Not only would we be able to evaluate the quality and effectiveness of cartilage healing, but we would also be able to evaluate the safety of implanting genetically modified MdChs within the body long-term. We also have the potential to investigate cartilage healing in an environment with mineralization. Basic calcium phosphate (BCP) crystals injected into rat knees induces osteoarthritis and upregulates inflammatory factors[47]. This model will allow us to evaluate multiple MdCh limiting factors for cartilage repair. Additionally, animal models will provide insight into the integrity of cartilage tissue with consistent loading.

BIBLIOGRAPHY

1. Sophia Fox, A. J., Bedi, A. & Rodeo, S. A. The basic science of articular cartilage: Structure, composition, and function. *Sports Health* **1**, 461–468 (2009).

2. Buckwalter, J. A. Articular cartilage injuries. *Clin Orthop Relat Res* 21–37 (2002) doi:10.1097/00003086-200209000-00004.

3. Holyoak, D. T., Tian, Y. F., van der Meulen, M. C. H. & Singh, A. Osteoarthritis: Pathology, Mouse Models, and Nanoparticle Injectable Systems for Targeted Treatment. *Annals of Biomedical Engineering* vol. 44 2062–2075 Preprint at https://doi.org/10.1007/s10439-016-1600-z (2016).

4. Hinoi, E. *et al.* Runx2 inhibits chondrocyte proliferation and hypertrophy through its expression in the perichondrium. *Genes Dev* **20**, 2937–2942 (2006).

5. Jiang, Y. & Tuan, R. S. Origin and function of cartilage stem/progenitor cells in osteoarthritis. *Nature Reviews Rheumatology* vol. 11 206–212 Preprint at https://doi.org/10.1038/nrrheum.2014.200 (2015).

6. Bekkers, J. E. J., Creemers, L. B., Dhert, W. J. A. & Saris, D. B. F. Diagnostic modalities for diseased articular cartilage-from defect to degeneration: A review. *Cartilage* **1**, 157–164 (2010).

7. Anderson, D. D. *et al.* Post-traumatic osteoarthritis: Improved understanding and opportunities for early intervention. *Journal of Orthopaedic Research* **29**, 802–809 (2011).

8. Thomas, A. C., Hubbard-turner, T., Wikstrom, E. A. & Palmieri-smith, R. M. Epidemiology of Posttraumatic Osteoarthritis. **52**, 491–496 (2017).

9. Thomas, A. C., Hubbard-Turner, T., Wikstrom, E. A. & Palmieri-Smith, R. M. Epidemiology of posttraumatic osteoarthritis. *Journal of Athletic Training* vol. 52 491–496 Preprint at https://doi.org/10.4085/1062-6050-51.5.08 (2017).

10. Kramer, W., Hendricks, K. & Wang, J. *Pathogenetic mechanisms of posttraumatic osteoarthritis: opportunities for early intervention*. www.ijcem.com (2011).

11. Kwon, H. *et al.* Surgical and tissue engineering strategies for articular cartilage and meniscus repair. *Nature Reviews Rheumatology* vol. 15 550–570 Preprint at https://doi.org/10.1038/s41584-019-0255-1 (2019).

12. Zylińska, B., Silmanowicz, P., Sobczyńska-Rak, A., Jarosz, Ł. & Szponder, T. Treatment of articular cartilage defects: Focus on tissue engineering. *In Vivo* vol. 32 1289–1300 Preprint at https://doi.org/10.21873/invivo.11379 (2018).

13. Song, S. J. & Park, C. H. Microfracture for cartilage repair in the knee: current concepts and limitations of systematic reviews. *Ann Transl Med* **7**, S108–S108 (2019).

14. Makris, E. A., Gomoll, A. H., Malizos, K. N., Hu, J. C. & Athanasiou, K. A. Repair and tissue engineering techniques for articular cartilage. *Nature Reviews Rheumatology* vol. 11 21–34 Preprint at https://doi.org/10.1038/nrrheum.2014.157 (2015).

15. Armiento, A. R., Alini, M. & Stoddart, M. J. Articular fibrocartilage - Why does hyaline cartilage fail to repair? *Advanced Drug Delivery Reviews* vol. 146 289–305 Preprint at https://doi.org/10.1016/j.addr.2018.12.015 (2019).

16. Paul, J. *et al.* Donor-site morbidity after osteochondral autologous transplantation for lesions of the talus. *Journal of Bone and Joint Surgery - Series A* **91**, 1683–1688 (2009).

17. Ma, B. *et al.* Gene expression profiling of dedifferentiated human articular chondrocytes in monolayer culture. *Osteoarthritis Cartilage* **21**, 599–603 (2013).

18. Mansour, J. M. Biomechanics of Cartilage. *Kinesiology: the mechanics and pathomechanics of human movement* 66–79 (2009) doi:10.1002/art.23548.

19. Little, C. J., Bawolin, N. K. & Chen, X. Mechanical properties of natural cartilage and tissue-engineered constructs. *Tissue Eng Part B Rev* **17**, 213–227 (2011).

20. Farrell, M. J. *et al.* Functional properties of bone marrow-derived MSC-based engineered cartilage are unstable with very long-term in vitro culture. *J Biomech* **47**, 2173–82 (2014).

21. Carrion, B. *et al.* The Synergistic Effects of Matrix Stiffness and Composition on the Response of Chondroprogenitor Cells in a 3D Precondensation Microenvironment. *Adv Healthc Mater* **5**, 1192–1202 (2016).

22. Khan, W. S., Adesida, A. B. & Hardingham, T. E. Hypoxic conditions increase hypoxia-inducible transcription factor 2α and enhance chondrogenesis in stem cells from the infrapatellar fat pad of osteoarthritis patients. *Arthritis Res Ther* **9**, (2007).

23. Das, R. H. J. *et al.* In vitro expansion affects the response of chondrocytes to mechanical stimulation. *Osteoarthritis Cartilage* **16**, 385–391 (2008).

24. Mackay, A. M. *et al. Chondrogenic Differentiation of Cultured Human Mesenchymal Stem Cells from Marrow*. *TISSUE ENGINEERING* vol. 4 www.liebertpub.com (1998).

25. Johnstone, B., Hering, T. M., Caplan, A. I., Goldberg, V. M. & Yoo, J. U. In vitro chondrogenesis of bone marrow-derived mesenchymal progenitor cells. *Exp Cell Res* **238**, 265–272 (1998).

26. Baksh, D., Song, L. & Tuan, R. S. Adult mesenchymal stem cells: characterization, differentiation, and application in cell and gene therapy. *J Cell Mol Med* **8**, 301–316 (2004).

27. Borrelli, J. *et al.* Understanding Articular Cartilage Injury and Potential Treatments. *J Orthop Trauma* **33**, S6–S11 (2019).

28. Bhosale, A. M. & Richardson, J. B. Articular cartilage: Structure, injuries and review of management. *British Medical Bulletin* vol. 87 77–95 Preprint at https://doi.org/10.1093/bmb/ldn025 (2008).

29. Xie, M. *et al.* Dynamic loading enhances chondrogenesis of human chondrocytes within a biodegradable resilient hydrogel. *Biomater Sci* **9**, 5011–5024 (2021).

30. Sorrell, J. M., Somoza, R. A. & Caplan, A. I. Human mesenchymal stem cells induced to differentiate as chondrocytes follow a biphasic pattern of extracellular matrix production. *Journal of Orthopaedic Research* **36**, 1757–1766 (2018).

31. Zha, K. *et al.* Heterogeneity of mesenchymal stem cells in cartilage regeneration: from characterization to application. *npj Regenerative Medicine* vol. 6 Preprint at https://doi.org/10.1038/s41536-021-00122-6 (2021).

32. Kim, J. & Adachi, T. Cell-fate decision of mesenchymal stem cells toward osteocyte differentiation is committed by spheroid culture. *Sci Rep* **11**, (2021).

33. Scotti, C. *et al.* Recapitulation of endochondral bone formation using human adult mesenchymal stem cells as a paradigm for developmental engineering. *Proc Natl Acad Sci U S A* **107**, 7251–7256 (2010).

34. Kronenberg, H. M. *Developmental regulation of the growth plate*. www.nature.com/nature (2003).

35. Akiyama, H., Chaboissier, M. C., Martin, J. F., Schedl, A. & de Crombrugghe, B. The transcription factor Sox9 has essential roles in successive steps of the chondrocyte differentiation pathway and is required for expression of Sox5 and Sox6. *Genes Dev* **16**, 2813–2828 (2002).

36. Vimalraj, S., Arumugam, B., Miranda, P. J. & Selvamurugan, N. Runx2: Structure, function, and phosphorylation in osteoblast differentiation. *International Journal of Biological Macromolecules* vol. 78 202–208 Preprint at https://doi.org/10.1016/j.ijbiomac.2015.04.008 (2015).

37. Penido, M. G. M. G. & Alon, U. S. Phosphate homeostasis and its role in bone health. *Pediatric Nephrology* vol. 27 2039–2048 Preprint at https://doi.org/10.1007/s00467-012-2175-z (2012).

38. Nalbant, S. *et al.* Synovial fluid features and their relations to osteoarthritis severity: New findings from sequential studies. *Osteoarthritis Cartilage* **11**, 50–54 (2003).

39. Ea, H. K. *et al.* Pathogenic Role of Basic Calcium Phosphate Crystals in Destructive Arthropathies. *PLoS One* **8**, (2013).

40. Corr, E. M., Cunningham, C. C., Helbert, L., McCarthy, G. M. & Dunne, A. Osteoarthritis-associated basic calcium phosphate crystals activate membrane proximal kinases in human innate immune cells. *Arthritis Res Ther* **19**, (2017).

41. Kim, D. H. & Rossi, J. J. RNAi mechanisms and applications. *BioTechniques* vol. 44 613–616 Preprint at https://doi.org/10.2144/000112792 (2008).

42. Guilak, F. *et al.* Designer Stem Cells: Genome Engineering and the Next Generation of Cell-Based Therapies. *Journal of Orthopaedic Research* **37**, 1287–1293 (2019).

43. Meerbrey, K. L. *et al.* The pINDUCER lentiviral toolkit for inducible RNA interference in vitro and in vivo. *Proc Natl Acad Sci U S A* **108**, 3665–70 (2011).

44. Moffat, J. *et al.* A Lentiviral RNAi Library for Human and Mouse Genes Applied to an Arrayed Viral High-Content Screen. *Cell* **124**, 1283–1298 (2006).

45. Guerrero, F. *et al.* TGF-β prevents phosphate-induced osteogenesis through inhibition of BMP and Wnt/β-catenin pathways. *PLoS One* **9**, (2014).

46. Wu, B. *et al.* Phosphate regulates chondrogenesis in a biphasic and maturation-dependent manner. *Differentiation* **95**, 54–62 (2017).

47. Stack, J. & McCarthy, G. Basic calcium phosphate crystals and osteoarthritis pathogenesis: Novel pathways and potential targets. *Current Opinion in Rheumatology* vol. 28 122–126 Preprint at https://doi.org/10.1097/BOR.0000000000000245 (2016).

48. Jung, Y. K. *et al.* Calcium-phosphate complex increased during subchondral bone remodeling affects earlystage osteoarthritis. *Sci Rep* **8**, (2018).

49. Wu, B., Kaur, G., Murali, S., Lanigan, T. & Coleman, R. M. A Synthetic, Closed-Looped Gene Circuit for the Autonomous Regulation of RUNX2 Activity during Chondrogenesis. doi:10.1101/2021.04.20.440669.

50. Mackay, A. M. *et al.* Chondrogenic differentiation of cultured human mesenchymal stem cells from marrow. *Tissue Eng* **4**, 415–428 (1998).

51. van der Kraan, P. M. & van den Berg, W. B. Chondrocyte hypertrophy and osteoarthritis: Role in initiation and progression of cartilage degeneration? *Osteoarthritis and Cartilage* vol. 20 223–232 Preprint at https://doi.org/10.1016/j.joca.2011.12.003 (2012).

52. Goldring, M. B. & Otero, M. Inflammation in osteoarthritis. *Current Opinion in Rheumatology* vol. 23 471–478 Preprint at https://doi.org/10.1097/BOR.0b013e328349c2b1 (2011).

53. Westendorf, J. J. & van Wijnen, A. J. Osteoporosis and osteoarthritis. *Osteoporosis and Osteoarthritis* 1–211 (2014) doi:10.1007/978-1-4939-1619-1.

54. Liu, Y. Z., Jackson, A. P. & Cosgrove, S. D. Contribution of calcium-containing crystals to cartilage degradation and synovial inflammation in osteoarthritis. *Osteoarthritis Cartilage* **17**, 1333–1340 (2009).

55. Newton, P. T. *et al.* Chondrogenic ATDC5 cells: An optimised model for rapid and physiological matrix mineralisation. *Int J Mol Med* **30**, 1187–1193 (2012).

56. Chung, C.-H., Golub, E. E., Forbes, E., Tokuoka, T. & Shapiro, I. M. *Calcified Tissue International Mechanism of Action of I-Glycerophosphate on Bone Cell Mineralization*. *Calcif Tissue Int* vol. 51 (1992).

57. Park, H. M., Lee, J. H. & Lee, Y. J. Positive association of serum alkaline phosphatase level with severe knee osteoarthritis: A nationwide population-based study. *Diagnostics* **10**, (2020).

58. Bertrand, J. *et al.* BCP crystals promote chondrocyte hypertrophic differentiation in OA cartilage by sequestering Wnt3a. *Ann Rheum Dis* **79**, 975–984 (2020).

59. Ea, H. K. *et al.* Pathogenic Role of Basic Calcium Phosphate Crystals in Destructive Arthropathies. *PLoS One* **8**, (2013).

60. Stücker, S., Bollmann, M., Garbers, C. & Bertrand, J. The role of calcium crystals and their effect on osteoarthritis pathogenesis. *Best Practice and Research: Clinical Rheumatology* vol. 35 Preprint at https://doi.org/10.1016/j.berh.2021.101722 (2021).

61. Magne, D. *et al. Phosphate Is a Specific Signal for ATDC5 Chondrocyte Maturation and Apoptosis-Associated Mineralization: Possible Implication of Apoptosis in the Regulation of Endochondral Ossification*. *J Bone Miner Res* vol. 18 (2003).

62. Somoza, R. A. *et al.* Transcriptome-Wide Analyses of Human Neonatal Articular Cartilage and Human Mesenchymal Stem Cell-Derived Cartilage Provide a New Molecular Target for Evaluating Engineered Cartilage. *Tissue Eng Part A* **24**, 335–350 (2018).

63. Mueller, M. B. & Tuan, R. S. Functional characterization of hypertrophy in chondrogenesis of human mesenchymal stem cells. *Arthritis Rheum* **58**, 1377–1388 (2008).

64. Kimata, M. *et al.* Signaling of extracellular inorganic phosphate up-regulates cyclin D1 expression in proliferating chondrocytes via the Na+/Pi cotransporter Pit-1 and Raf/MEK/ERK pathway. *Bone* **47**, 938–947 (2010).

65. Medvedeva, E. v. *et al.* Repair of damaged articular cartilage: Current approaches and future directions. *Int J Mol Sci* **19**, (2018).

66. Song, S. J. & Park, C. H. Microfracture for cartilage repair in the knee: current concepts and limitations of systematic reviews. *Ann Transl Med* **7**, S108–S108 (2019).

67. Makris, E. A., Gomoll, A. H., Malizos, K. N., Hu, J. C. & Athanasiou, K. A. Repair and tissue engineering techniques for articular cartilage. *Nature Reviews Rheumatology* vol. 11 21–34 Preprint at https://doi.org/10.1038/nrrheum.2014.157 (2015).

68. Dewan, A. K., Gibson, M. A., Elisseeff, J. H. & Trice, M. E. Evolution of autologous chondrocyte repair and comparison to other cartilage repair techniques. *BioMed Research International* vol. 2014 Preprint at https://doi.org/10.1155/2014/272481 (2014).

69. Darling, E. M. & Athanasiou, K. A. Rapid phenotypic changes in passaged articular chondrocyte subpopulations. *Journal of Orthopaedic Research* **23**, 425–432 (2005).

70. Visweswaran, M. *et al.* Multi-lineage differentiation of mesenchymal stem cells - To Wnt, or not Wnt. *International Journal of Biochemistry and Cell Biology* vol. 68 139–147 Preprint at https://doi.org/10.1016/j.biocel.2015.09.008 (2015).

71. Sophia Fox, A. J., Bedi, A. & Rodeo, S. A. The basic science of articular cartilage: Structure, composition, and function. *Sports Health* **1**, 461–468 (2009).

72. Khan, W. S., Adesida, A. B. & Hardingham, T. E. Hypoxic conditions increase hypoxia-inducible transcription factor 2α and enhance chondrogenesis in stem cells from the infrapatellar fat pad of osteoarthritis patients. *Arthritis Res Ther* **9**, (2007).

73. Kanichai, M., Ferguson, D., Prendergast, P. J. & Campbell, V. A. Hypoxia promotes chondrogenesis in rat mesenchymal stem cells: A role for AKT and hypoxia-inducible factor (HIF)-1α. *J Cell Physiol* **216**, 708–715 (2008).

74. Murphy, C. L. & Polak, J. M. Control of Human Articular Chondrocyte Differentiation by Reduced Oxygen Tension. *J Cell Physiol* **199**, 451–459 (2004).

75. Monfort, J. *et al.* Decreased metalloproteinase production as a response to mechanical pressure in human cartilage: A mechanism for homeostatic regulation. *Arthritis Res Ther* **8**, (2006).

76. Wu, B., Kaur, G., Murali, S., Lanigan, T. & Coleman, R. M. A Synthetic, Closed-Looped Gene Circuit for the Autonomous Regulation of RUNX2 Activity during Chondrogenesis. *bioRxiv* 2021.04.20.440669 (2021) doi:10.1101/2021.04.20.440669.

77. Mccarty, W. J., Pallante, A. L., Rone, R. J., Bugbee, W. D. & Sah, R. L. *The Proteoglycan Metabolism of Articular Cartilage in Joint-Scale Culture*. www.liebertonline.com=ten.

78. Mueller, M. B. & Tuan, R. S. Functional characterization of hypertrophy in chondrogenesis of human mesenchymal stem cells. *Arthritis Rheum* **58**, 1377–1388 (2008).

79. Almalki, S. G. & Agrawal, D. K. Effects of matrix metalloproteinases on the fate of mesenchymal stem cells. *Stem Cell Research and Therapy* vol. 7 Preprint at https://doi.org/10.1186/s13287-016-0393-1 (2016).

80. Behonick, D. J. *et al.* Role of matrix metalloproteinase 13 in both endochondral and intramembranous ossification during skeletal regeneration. *PLoS One* **2**, (2007).

81. Athanasiou, K. A., Rosenwasser, M. P., Buckwalter, J. A., Malinin, T. I. & Mow, V. C. Interspecies comparisons of in situ intrinsic mechanical properties of distal femoral cartilage. *Journal of Orthopaedic Research* **9**, 330–340 (1991).

82. Lee, H. H. *et al.* Hypoxia enhances Chondrogenesis and prevents terminal differentiation through pi3k/akt/foxo dependent anti-Apoptotic effect. *Sci Rep* **3**, (2013).

83. Huang, A. H., Farrell, M. J. & Mauck, R. L. Mechanics and mechanobiology of mesenchymal stem cell-based engineered cartilage. *J Biomech* **43**, 128–136 (2010).

84. Chen, H. *et al.* Runx2 regulates endochondral ossification through control of chondrocyte proliferation and differentiation. *Journal of Bone and Mineral Research* **29**, 2653–2665 (2014).

85. Bellows, C. G., Heersche, J. N. M. & Aubin, J. E. Inorganic phosphate added exogenously or released from B-glycerophosphate initiates mineralization of osteoid nodules in vitro. *Bone Miner* 15–29 (1992).

86. Wang, X. *et al. The MEK-ERK1/2 signaling pathway regulates hyaline cartilage formation and the redifferentiation of dedifferentiated chondrocytes in vitro*. *Am J Transl Res* vol. 10 www.ajtr.org/ISSN:1943-8141/AJTR0076680 (2018).

87. Chang, S. H. *et al.* Elevated inorganic phosphate stimulates Akt ERK1/2-Mnk1 signaling in human lung cells. *Am J Respir Cell Mol Biol* **35**, 528–539 (2006).

88. Rui, S. *et al.* Phosphate promotes osteogenic differentiation through non-canonical Wnt signaling pathway in human mesenchymal stem cells. *Bone* **164**, (2022).

89. Bertrand, J. *et al.* BCP crystals promote chondrocyte hypertrophic differentiation in OA cartilage by sequestering Wnt3a. *Ann Rheum Dis* **79**, 975–984 (2020).

90. Nasi, S., So, A., Combes, C., Daudon, M. & Busso, N. Interleukin-6 and chondrocyte mineralisation act in tandem to promote experimental osteoarthritis. *Ann Rheum Dis* **75**, 1372–1379 (2016).

91. Hu, J. C. & Athanasiou, K. A. A Self-Assembling Process in Articular Cartilage Tissue Engineering. *Tissue Eng* **12**, 969–979 (2006).

92. Pattappa, G., Zellner, J., Johnstone, B., Docheva, D. & Angele, P. Cells under pressure - the relationship between hydrostatic pressure and mesenchymal stem cell chondrogenesis. *European cells & materials* vol. 37 360–381 Preprint at https://doi.org/10.22203/eCM.v037a22 (2019).

93. Dickhut, A., Gottwald, E., Steck, E., Heisel, C. & Richter, W. *Chondrogenesis of mesenchymal stem cells in gel-like biomaterials in vitro and in vivo*. *Frontiers in Bioscience* vol. 13 (2008).

94. Woods, A., Wang, G. & Beier, F. Regulation of chondrocyte differentiation by the act in cytoskeleton and adhesive interactions. *Journal of Cellular Physiology* vol. 213 1–8 Preprint at https://doi.org/10.1002/jcp.21110 (2007).

95. Boeuf, S. & Richter, W. Chondrogenesis of mesenchymal stem cells: role of tissue source and inducing factors. *Stem Cell Res Ther* (2010).

96. Charalambous, C. P. Articular cartilage. Part II: Degeneration and osteoarthrosis, repair, regeneration, and transplantation. *Classic Papers in Orthopaedics* 389–391 Preprint at https://doi.org/10.1007/978-1-4471-5451-8_98 (2014).

97. Weissenberger, M. *et al.* Reduced hypertrophy in vitro after chondrogenic differentiation of adult human mesenchymal stem cells following adenoviral SOX9 gene delivery. *BMC Musculoskelet Disord* **21**, (2020).

98. Pferdehirt, L., Ross, A. K., Brunger, J. M. & Guilak, F. A Synthetic Gene Circuit for Self-Regulating Delivery of Biologic Drugs in Engineered Tissues. *Tissue Eng Part A* **25**, 809–820 (2019).

99. Murphy, C. L., Thoms, B. L., Vaghjiani, R. J. & Lafont, J. E. Hypoxia. HIF-mediated articular chondrocyte function: prospects for cartilage repair. *Arthritis research & therapy* vol. 11 213 Preprint at https://doi.org/10.1186/ar2574 (2009).

100. Thoms, B. L., Dudek, K. A., Lafont, J. E. & Murphy, C. L. Hypoxia Promotes the Production and Inhibits the Destruction of Human Articular Cartilage. *Arthritis Rheum* **65**, 1302–1312 (2013).

101. Markway, B. D., Cho, H. & Johnstone, B. Hypoxia promotes redifferentiation and suppresses markers of hypertrophy and degeneration in both healthy and osteoarthritic chondrocytes. *Arthritis Res Ther* **15**, (2013).

102. Saadat, E., Lan, H., Majumdar, S., Rempel, D. M. & King, K. B. Long-term cyclical in vivo loading increases cartilage proteoglycan content in a spatially specific manner: An infrared microspectroscopic imaging and polarized light microscopy study. *Arthritis Res Ther* **8**, (2006).

103. Bachmann, B. *et al.* Stiffness Matters: Fine-Tuned Hydrogel Elasticity Alters Chondrogenic Redifferentiation. *Front Bioeng Biotechnol* **8**, (2020).

104. Park, J. S. *et al.* The effect of matrix stiffness on the differentiation of mesenchymal stem cells in response to TGF-β. *Biomaterials* **32**, 3921–3930 (2011).

105. Han, S. B., Kim, J. K., Lee, G. & Kim, D. H. Mechanical Properties of Materials for Stem Cell Differentiation. *Adv Biosyst* **4**, (2020).

106. Mouw, J. K., Case, N. D., Guldberg, R. E., Plaas, A. H. K. & Levenston, M. E. Variations in matrix composition and GAG fine structure among scaffolds for cartilage tissue engineering. *Osteoarthritis Cartilage* **13**, 828–836 (2005).

107. Horner, C. B., Low, K. & Nam, J. Electrospun Scaffolds for Cartilage Regeneration. in *Nanocomposites for Musculoskeletal Tissue Regeneration* 213–240 (Elsevier Inc., 2016). doi:10.1016/B978-1-78242-452-9.00010-8.

108. Yilmaz, E. N. & Zeugolis, D. I. Electrospun Polymers in Cartilage Engineering—State of Play. *Frontiers in Bioengineering and Biotechnology* vol. 8 Preprint at https://doi.org/10.3389/fbioe.2020.00077 (2020).

109. Holmes, B., Castro, N. J., Zhang, L. G. & Zussman, E. Electrospun fibrous scaffolds for bone and cartilage tissue generation: Recent progress and future developments. *Tissue Eng Part B Rev* **18**, 478–486 (2012).

110. Gregory, M. H. *et al.* A Review of Translational Animal Models for Knee Osteoarthritis. **2012**, (2012).

111. Kuyinu, E. L., Narayanan, G., Nair, L. S. & Laurencin, C. T. Animal models of osteoarthritis: Classification, update, and measurement of outcomes. *J Orthop Surg Res* **11**, 1–27 (2016).

112. Katagiri, H., Mendes, L. F. & Luyten, F. P. Definition of a Critical Size Osteochondral Knee Defect and its Negative Effect on the Surrounding Articular Cartilage in the Rat. *Osteoarthritis Cartilage* **25**, 1531–1540 (2017).

113. Goebel, J. C. *et al.* High-resolution MRI (7T) of femoro-tibial cartilage changes in the rat anterior cruciate ligament transection model of osteoarthritis: A cross-sectional study. *Rheumatology* **49**, 1654–1664 (2010).

114. Marlovits, S. *et al.* Magnetic resonance observation of cartilage repair tissue (MOCART) for the evaluation of autologous chondrocyte transplantation: Determination of interobserver variability and correlation to clinical outcome after 2 years. *Eur J Radiol* **57**, 16–23 (2006).